

# On the Benefits of Network-Level Cooperation in Millimeter-Wave Communications

Cristian Tatino, *Student Member, IEEE*, Nikolaos Pappas, *Member, IEEE*,  
Ilaria Malanchini, *Member, IEEE*, Lutz Ewe, and Di Yuan, *Senior Member, IEEE*

## Abstract

Relaying techniques for millimeter-wave wireless networks represent a powerful solution for improving the transmission performance. In this work, we quantify the benefits in terms of delay and throughput for a random-access multi-user millimeter-wave wireless network, assisted by a full-duplex network cooperative relay. The relay is equipped with a queue for which we analyze the performance characteristics (e.g., arrival rate, service rate, average size, and stability condition). Moreover, we study two possible transmission schemes: fully directional and broadcast. In the former, the source nodes transmit a packet either to the relay or to the destination by using narrow beams, whereas, in the latter, the nodes transmit to both the destination and the relay in the same timeslot by using a wider beam, but with lower beamforming gain. In our analysis, we also take into account the beam alignment phase that occurs every time a transmitter node changes the destination node. We show how the beam alignment duration, as well as position and number of transmitting nodes, significantly affect the network performance. Moreover, we illustrate the optimal transmission scheme (i.e., broadcast or fully directional) for several system parameters and show that a fully directional transmission is not always beneficial, but, in some scenarios, broadcasting and relaying can improve the performance in terms of throughput and delay.

## Index Terms

Millimeter-waves, network cooperative relaying, beam alignment, random access networks, directional communications.

This work extends the preliminary study in [1]. This project has received funding from the European Union’s Horizon 2020 research and innovation programme under the Marie Skłodowska-Curie grant agreement No. 643002.

## I. INTRODUCTION

In the recent years, millimeter-wave (mm-wave) communications have attracted the interest of many researchers, who see the abundance of spectrum resource in the mm-wave frequency range (30-300 GHz) as a possible solution to the longstanding problem of spectrum scarcity. For this reason, mm-wave wireless networks have been identified as one of the key enabler technologies for the next generation of mobile communications, i.e., 5G [2]. Although mm-waves communications can reach tremendous high data rates [3], the signal propagation is subject to higher path loss and penetration loss [4], [5], in comparison to lower frequency communications. Such high losses cause frequent interruptions, especially when obstacles block the signal path [6]. Directional communications and narrow beams provide high beamforming gains that contribute to mitigate the path loss issue. By using narrow beams, the transmitters focus the signal energy along only few directions and paths and, usually, the line-of-sight (LOS) path is characterized by the lowest path loss [4], [5]. When the LOS path is blocked by an obstacle, the use of reflected transmission paths can overcome the blockage issue [7].

Other solutions for avoiding interruptions caused by blockages provide alternative transmission paths by using additional nodes, e.g., multi-connectivity [8], [9] and relaying techniques. In the latter, a source node (user equipment, UE) transmit a packet to an intermediate node (relay) when the source-destination path is blocked. Though relaying has been extensively analyzed for microwave frequencies [10]–[17], mm-wave communications present some peculiarities, such as the use of narrow beams and the beam alignment phase, that make further analysis necessary. For instance, by using narrow beams the UE might not be able to transmit simultaneously to both the relay and the destination node, which is usually the case with omnidirectional transmissions at lower frequencies. By using narrow beams in mm-waves, in each timeslot the UE may transmit a packet either to the destination or the relay. Moreover, every time the UEs change the receiver (i.e., from the destination to the relay and vice-versa), a new beam alignment might be required [18], [19]. This can both cause further delays and affect the throughput.

In this work, we propose a novel analysis of network-level cooperative communications in mm-wave wireless networks with a mm-wave access point (mmAP) as transmission target and one network cooperative full-duplex relay that is equipped with a queue. We analyze the impact of directional communications by evaluating two possible transmission schemes, i.e., broadcast (BR) and fully directional (FD). By using the former, the UEs transmit simultaneously to both

the mmAP and the relay by means of wider beams at lower beamforming gains, whereas, with the FD scheme, the UEs transmit either to the mmAP or to the relay by using narrow beams. Moreover, we take into account the beam alignments that occur every time the transmitters change receiver and scheme.

### A. Related Work

Several works have been proposed for evaluating the benefits of relaying techniques in mm-wave communications, e.g., [20]–[29]. In [20], the authors propose a physical layer analysis of cooperative communications for frequencies above 10 GHz and evaluate the outage probability of several multiple access protocols, combining techniques, and relay transmission techniques. The study in [20] shows that the use of relays drastically improves the coverage probability and the correlation between the source-relay and relay-destination links can be exploited to improve the performance. The authors of [21], [22] use stochastic geometry to show the improvements in the signal-to-interference-plus-noise ratio (SINR) distribution and coverage probability for a mm-wave cellular network that is assisted by a relay. Moreover, the results of [22] show the asymptotic gain that can possibly be achieved by using the best relay selection strategy with respect to a random relay selection approach.

Stochastic geometry is also used in [23]–[26]. In [23], the connection probability for mm-wave wireless networks with multi-hop relaying is analyzed. The authors show that the connection probability is strictly correlated to the obstacle density and the width of the region where the relays are potentially selected. In [24], the coverage probability for a decode-and-forward relay is analyzed; the authors consider the relay that has the highest signal-to-noise ratio (SNR) to the receiver among the set of relays that can decode the source message. In [25] and [26], the authors focus on relaying techniques for device-to-device (D2D) scenarios and analyze, by using stochastic geometry, the coverage probability and the relay selection problem, respectively. The relay selection strategy is further evaluated in [27], [28]. The former proposes a two-hop relay selection algorithm for mm-wave communications to take into account the dependency between the source-destination and relay-destination paths in terms of line-of-sight (LOS) probability. The work in [28] considers a joint relay selection and mmAP association problem. In particular, the authors propose a distributed solution that takes into account the load balancing and fairness aspects among multiple mmAPs.

None of the aforementioned studies considers the beam alignment phase. This aspect is taken into account in [29], where a single source-destination pair and a single half-duplex relay scenario is considered. Namely, when the source-destination link is blocked, the source node can transmit either to the relay by using mm-waves or to both the relay and the destination by using lower frequencies. In the former case a beam alignment occurs. The authors compare the two approaches in terms of throughput and delay, but differently from our approach they assume continuous time and single UE scenario.

In general, analysis of relaying techniques in mm-wave wireless networks regarding network-level performance need further studies. However, it is worth mentioning works that propose similar analysis for lower frequencies, such as [15], [16]. In [15], the authors consider a multi-user scenario with a full-duplex relay and a destination that have multi-packet reception capability, whereas, the studies in [16], [30] analyze a similar scenario, but with two relays. In [15], [16], [30], the relays are equipped with infinite size queue for which the performance are analyzed as well as the per-user and network throughput, and the delay per packet. Buffer-aided relays are also considered by [17] that illustrates and compares several relay selection techniques for lower frequencies wireless networks.

### *B. Contributions*

We provide a novel analysis of delay and throughput for random access multi-user cooperative relaying mm-wave wireless networks. We show the tradeoff between using the aforementioned transmission schemes, i.e., FD and BR, by taking into account the different beamforming gains and interference caused by both types of transmissions. Namely, in contrast to the FD scheme, BR transmissions use wider beams that provide a lower beamforming gain, but they can allow to transmit simultaneously both to the relay and the mmAP. Furthermore, switching transmission scheme involves a beam alignment phase between the transmitter and the receiver and, therefore, we show how the duration of this phase impacts the performance.

In more detail, at first, we compute the analytical expression of the user transmit probability, which, as we show, is decreased by the beam alignment. Then, by using queueing theory, we study the performance characteristics of the queue at the relay, for which we derive the stability condition, as well as the service and the arrival rate. Finally, we identify the optimal transmission scheme (i.e., FD and BR) with respect to several system parameters, e.g., number and positions of nodes, and beam alignment duration. Namely, we investigate when it is more beneficial for

the UEs to transmit simultaneously to both the mmAP and the relay by using wider beams, and when instead it is better to use narrow beams and transmit either to the mmAP or the relay. To the best of our knowledge, such analysis has not been investigated yet.

The rest of the paper is organized as follows: In Section II, we describe the system model and the assumptions. In Section III, we present the queue analysis at the relay with two UEs. These results are then generalized in Section IV-A, where we evaluate the aggregate network throughput for  $N$  UEs, for which, in Section IV-B we derive the delay per packet expression. In Section V, we illustrate the results and performance evaluation and Section VI concludes the paper.

## II. SYSTEM MODEL AND ASSUMPTIONS

### A. Network Model

We consider a set  $\mathcal{N}$ , with cardinality  $N$ , of symmetric<sup>1</sup> UEs, which are characterized by the same mm-wave networking characteristics such as propagation conditions and topology. We assume multiple packet reception capability both at the mmAP and the relay ( $R$ ), which are equipped with hybrid beamformers so they can form multiple beams at the same time for multiple packets reception [31]. Each UE however is considered to be equipped with an analog beamformer and it can form only one beam at a time. We assume slotted time and each packet transmission takes one timeslot. The relay has no packets of its own, but it stores the successfully received packets from the UEs in a queue, which has infinite size. The UEs have saturated queues, i.e., they never empty. We assume that acknowledgements (ACKs) are instantaneous and error free<sup>2</sup> and successfully received packets are removed from the queues of the transmitting nodes, i.e., both the UEs and  $R$ .

In a given timeslot, the relay transmits a packet to the mmAP with probability  $q_r$ , whereas, the UEs decide to transmit a packet with probability  $q_u$ . Then, the UEs randomly select one of the two transmission schemes, i.e., BR or FD, with probability  $q_{ub}$  and  $q_{uf}$ , respectively, with  $q_{uf} + q_{ub} = 1$ . If the UEs use a BR transmission and the transmission to the destination fails, the relay stores the packets (that are correctly decoded) in its queue and is responsible to transmit

<sup>1</sup>This study can be generalized to the asymmetric case; however, the analysis will be dramatically involved without providing any additional meaningful insight.

<sup>2</sup>The assumptions of error free ACK and infinite size queue are considered for the purpose of analysis that is still valid if the queue is large enough.

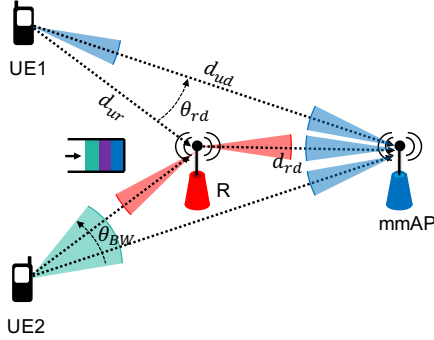


Fig. 1: FD (UE1) and BR (UE2) transmissions for a scenario with two UEs, one relay and one mmAP. In this example, UE1 is transmitting to the mmAP.

it to the destination. This technique is also known as network level cooperation relaying [11], [14]–[16]. In contrast, if the FD scheme is selected, then the UEs choose to transmit either to the relay, with probability  $q_{ur}$ , or to the mmAP, with probability  $q_{um}$ , where  $q_{ur} + q_{um} = 1$ .

We can summarize this process by defining the set of transmission strategies,  $\mathcal{S} = \{fm, fr, b\}$ , where,  $fm$ ,  $fr$  and  $b$  represent the cases in which a UE transmits to the mmAP, to  $R$ , and to both, respectively. Let  $P(s = i)$  be the probability of using strategy  $i$ , with  $i \in \mathcal{S}$ . These probabilities do not depend on the particular timeslot and are given by:  $P(s = fm) = q_{uf}q_{um}$ ,  $P(s = fr) = q_{uf}q_{ur}$  and  $P(s = b) = q_{ub}$ . If the selected strategy is the same as in the previous transmission attempt, then the UE can directly transmit, otherwise it has to perform a beam alignment. The alignment is done by the UEs every time they decide to transmit and change strategy. We assume that the beam alignment duration is independent from the selected strategy and equals to  $D_a$  timeslots and, while a UE is performing an alignment, it can not transmit. Thus, the probability that a UE is *actually* transmitting,  $q_{tx}$ , is affected by the beam alignment, and its derivation is presented in the next section.

In Fig. 1, we illustrate an example of the FD and BR transmissions, where  $d_{ur}$  and  $d_{ud}$  represent the distances of the paths UE- $R$  and UE-mmAP, respectively. The parameter  $\theta_{rd}$  is the angle formed by  $R$  and the mmAP with a UE as vertex and  $\theta_{BW}$  is the beamwidth. Hereafter, we indicate the probability of the complementary event by a bar over the term (e.g.,  $\bar{q}_u = 1 - q_u$ ). Moreover, we use superscripts  $f$  and  $b$  to indicate the FD and BR transmissions, respectively.

### B. SINR Expression and Success Probability

A packet is considered to be successfully received if the SINR is above a certain threshold  $\gamma$ . Ideally, multiple transmissions at the receiver side of a node do not interfere when they are received on different beams. However, in real scenarios, interference cancellation techniques are not perfect. Therefore, we introduce a coefficient  $0 \leq \alpha \leq 1$  that models the interference between received beams<sup>3</sup>. The cases  $\alpha = 0$  and  $\alpha = 1$  represent perfect interference cancellation and no interference cancellation, respectively. Moreover, given the negligible interference between transmissions of different pairs of nodes in mm-waves [32], we assume that an FD transmission to the mmAP does not interfere with the packet transmitted to  $R$  and vice-versa. On the other hand, when a UE uses a BR transmission, its transmission interferes with the transmissions of the other UEs for both the mmAP and  $R$ .

We assume that the links between all pairs of nodes are independent and can be in two different states, line-of-sight (LOS) and non-line-of-sight (NLOS). Specifically,  $\text{LOS}_{ij}$  and  $\text{NLOS}_{ij}$  are the events that node  $i$  is in LOS and NLOS with node  $j$ , respectively. The associated probabilities are denoted as  $P(\text{LOS}_{ij})$  and  $P(\text{NLOS}_{ij})$ . Note that, hereafter, we use subscripts  $i$  and  $j$  to indicate generic nodes, while,  $u$ ,  $r$ , and  $d$  to indicate the UEs, the relay, and the mmAP, respectively. Usually, relay  $R$  is chosen to be a node that is placed in a position that guarantees the LOS with the mmAP, therefore we assume that  $P(\text{LOS}_{rd}) = 1$ .

In order to compute the SINR for link  $ij$ , we first identify the sets of interferers that use FD and BR transmissions, which are  $\mathcal{I}_f$  and  $\mathcal{I}_b$ , respectively. Then, we partition each of them into the sets of nodes that are in LOS and NLOS with node  $j$ . These sets are  $\mathcal{I}_{fl}$  and  $\mathcal{I}_{fn}$ , for the nodes that use the FD transmission and  $\mathcal{I}_{bl}$  and  $\mathcal{I}_{bn}$  for the UEs that use the BR transmission. Thus, when node  $i$  is in LOS with node  $j$ , we can derive the SINR, conditioned to  $\mathcal{I}_{fl}$ ,  $\mathcal{I}_{fn}$ ,  $\mathcal{I}_{bl}$ ,  $\mathcal{I}_{bn}$ , as follows:

$$\begin{aligned} & \text{SINR}_{ij/\mathcal{I}_{fl},\mathcal{I}_{fn},\mathcal{I}_{bl},\mathcal{I}_{bn}}^f | \text{LOS}_{ij} \\ &= \frac{p_t g_i^f g_j^f h_l(i, j)}{p_N + \alpha \left( \sum_{k \in \mathcal{I}_{fl}} p_{r/l}^f(k, j) + \sum_{m \in \mathcal{I}_{bl}} p_{r/l}^b(m, j) + \sum_{u \in \mathcal{I}_{fn}} p_{r/n}^f(u, j) + \sum_{v \in \mathcal{I}_{bn}} p_{r/n}^b(v, j) \right)}, \end{aligned} \quad (1)$$

<sup>3</sup>Our work can be easily generalized to the case where  $\alpha$  depends on the transmission strategy. However, in order to keep the clarity of the presentation we consider  $\alpha$  to be constant.

TABLE I: Summary of the notation.

BR	broadcast transmission	FD	fully directional transmission
UE	user equipment	$N$	number of UEs
mmAP	mm-wave access point (destination)	$R$	relay
$D_a$	beam alignment delay	$q_r$	relay transmit probability
$q_u$	UE transmit probability	$q_{tx}$	<i>actual</i> UE transmit probability
$q_{ub}$	probability to use a BR transmission	$q_{uf}$	probability to use an FD transmission
$q_{um}$	probability to transmit to the mmAP when using FD transmissions	$q_{ur}$	probability to transmit to $R$ when using FD transmissions
$\mathcal{S}$	set of transmission strategies	$d_{dr}$	mmAP-relay distance
$d_{ud}$	UE-mmAP distance	$d_{ur}$	UE-relay distance
$\mathcal{I}_b$	set of interferers that use BR transmissions	$\mathcal{I}_f$	set of interferers that use FD transmissions
$\lambda_r$	arrival rate at the relay	$\mu_r$	service rate at the relay
$P_{ij/\mathcal{I}_f, \mathcal{I}_b}^b$	success probability of a transmission from the i-th to the j-th nodes by using a BR transmission	$P_{ij/\mathcal{I}_f, \mathcal{I}_b}^b$	success probability of a transmission from the i-th to the j-th nodes by using an FD transmission
$\theta_{rd}$	angle between the mmAP and $R$ with the UE as vertex	$\theta_{BW}$	beamwidth

where,  $g_i$  and  $g_j$  are the transmitter and receiver beamforming gains, respectively, and they are computed in according to the ideal sectored antenna model [33], which is given by:  $g_i = g_j = \frac{2\pi}{\theta_{BW}}$  in the main lobe, and 0 otherwise. The term  $h_l(i, j)$  is the path loss on link  $ij$  when this is in LOS. The transmit power and the noise power are  $p_t$  and  $p_N$ , respectively. The terms  $p_{r/l}(i, j)$  and  $p_{r/n}(i, j)$  represent the received power by node  $j$  from node  $i$ , when the first is in LOS and NLOS, respectively. Note that similar expressions of the SINR can be derived also in case of BR and NLOS.

Finally, the success probabilities for a packet sent on link  $ij$  by using FD and BR transmissions are represented by the terms  $P_{ij/\mathcal{I}_f, \mathcal{I}_b}^f$  and  $P_{ij/\mathcal{I}_f, \mathcal{I}_b}^b$ , respectively. Here, we consider only the conditioning on the sets  $\mathcal{I}_f$  and  $\mathcal{I}_b$  because we average on all the possible scenarios for the LOS and NLOS link conditions. The expression for the FD transmission and  $N$  UEs is given in Appendix A.

### III. PERFORMANCE ANALYSIS

#### A. UE Transmit Probability

In this section, we first derive the *actual* transmit probability of a UE in a given timeslot, i.e.,  $q_{tx}$ , when beam alignment is taken into account. Then, we evaluate the performance of the

queue at the relay and we analyze the network throughput and the delay per packet.

**Theorem 1.** *For each timeslot  $k$ , the probability distributions of the transmission strategy selection  $P(s_k = i)$  are i.d. with  $i \in \mathcal{S}$ , then, the transmit probability for a UE in a timeslot  $k$ , with constant alignment duration  $D_a$ , is given by:*

$$q_{tx} = P(I_k)q_u = \frac{q_u}{1 + D_a(1 - P(s_k = i \cap s_{\hat{k}} = i))}, \quad (2)$$

where,  $q_u$  is defined in Section II-A and  $P(I_k)$  is the probability that the UE has not started an alignment in the previous  $D_a$  timeslots. The term  $P(s_k = i \cap s_{\hat{k}} = i)$  is the probability to use the  $i$ -th strategy in timeslot  $k$  while using the same strategy for the previous transmission attempt, which occurs in the  $\hat{k}$ -th timeslot.

*Proof.* The proof is given in Appendix B.  $\square$

From (2), one can notice that  $q_{tx}$  is inversely proportional to the beam alignment duration  $D_a$  as well as to the probability of changing strategy  $1 - P(s_k = i \cap s_{\hat{k}} = i)$ . Assuming that the probabilities of the transmission strategy selection,  $P(s_k = i)$ , are independent in each timeslot  $k$  and have values as reported in Section II-A,  $P(I_k)$  can be written as:

$$P(I_k) = \frac{1}{1 + D_a q_u (1 - (q_{uf} q_{um})^2 - (q_{uf} q_{ur})^2 - (q_{ub})^2)}. \quad (3)$$

### B. Queue Analysis

In this section, we evaluate the arrival rate,  $\lambda_r$ , the service rate,  $\mu_r$ , and the stability condition for the queue at the relay  $R$ . For the sake of clarity, we first present hereafter the results for two UEs and then we generalize these for  $N$  UEs. First, we compute  $\lambda_r$  that can be expressed as follows:

$$\lambda_r = P(Q = 0)\lambda_r^0 + P(Q \neq 0)\lambda_r^1, \quad (4)$$

where  $\lambda_r^0$  and  $\lambda_r^1$  represent the arrival rate at  $R$  when the queue is empty or not empty. These two events occur with probabilities  $P(Q = 0)$  and  $P(Q \neq 0)$ , respectively. Indeed, when the queue is not empty,  $R$  may transmit and interfere with the other transmissions to the mmAP. This interference affects the number of received packets by the  $R$  when broadcast transmissions are used. In a two UE scenario,  $R$  will receive at maximum two packets per timeslot. By considering all the possible cases we can compute  $\lambda_r^0$  and  $\lambda_r^1$ . Moreover, for the

success probability expressions, we explicitly identify the nodes that belong to the sets  $\mathcal{I}_f$  and  $\mathcal{I}_b$ . In particular, since the UEs are symmetric, it is sufficient to indicate the number of UEs that are interfering and whether  $R$  is transmitting; i.e., we indicate with  $\{|\mathcal{I}_f|, r\}^f$  and  $\{|\mathcal{I}_f|\}^f$  the sets of interferers that use FD transmissions when  $R$  is transmitting or not, and with  $\{r\}^f$  the set of interferers when only the relay  $R$  is transmitting. Therefore, we obtain:

$$\begin{aligned} \lambda_r^0 = & 2q_{tx}\bar{q}_{tx}q_{uf}q_{ur}P_{ur}^f + 2q_{tx}\bar{q}_{tx}q_{ub}P_{ur}^b\bar{P}_{ud}^b \\ & + q_{tx}^2q_{uf}^2q_{ur}^2q_{ur}^2\left[2P_{ur/\{1\}^f}^f\bar{P}_{ur/\{1\}^f}^f + 2\left(P_{ur/\{1\}^f}^f\right)^2\right] + 2q_{tx}^2q_{uf}^2q_{ur}q_{um}P_{ur}^f \\ & + 2q_{tx}^2q_{1f}q_{ub}q_{ur}\left[P_{ur/\{1\}^b}^f\left(1 - P_{ur/\{1\}^f}^b\bar{P}_{ud}^b\right) + \bar{P}_{ur/\{1\}^b}^fP_{ur/\{1\}^f}^b\bar{P}_{ud}^b + 2\left(P_{ur/\{1\}^f}^b\bar{P}_{ud}^b\right)^2\right] \\ & + 2q_{tx}^2q_{ub}q_{uf}q_{um}P_{ur}^b\bar{P}_{ud/\{1\}^f}^b + q_{tx}^2q_{ub}^2\left[2P_{ur/\{1\}^b}^b\bar{P}_{ud/\{2\}^b}^b\left(1 - P_{ur/\{1\}^b}^b\bar{P}_{ud/\{1\}^b}^b\right)\right. \\ & \left.+ 2\left(P_{ur/\{1\}^b}^b\bar{P}_{ud/\{1\}^b}^b\right)^2\right], \end{aligned} \quad (5)$$

where,  $q_{tx}$ ,  $q_{ub}$ ,  $q_{uf}$ ,  $q_{ud}$ , and  $q_{ur}$  are introduced in Section II-A and a summary of the notation is available in Table I. The term  $\lambda_r^1$  can be written as  $\lambda_r^1 = \bar{q}_r\lambda_r^0 + q_rA_r$ , where  $A_r$  is given by:

$$\begin{aligned} A_r = & 2q_{tx}\bar{q}_{tx}q_{uf}q_{ur}P_{ur}^f + 2q_{tx}\bar{q}_{tx}q_{ub}P_{ur}^b\bar{P}_{ud}^b + q_{tx}^2q_{uf}^2q_{ur}^2q_{ur}^2\left[2P_{ur/\{1\}^f}^f\bar{P}_{ur/\{1\}^f}^f\right. \\ & \left.+ 2\left(P_{ur/\{1\}^f}^f\right)^2\right] + 2q_{tx}^2q_{uf}^2q_{ur}q_{um}P_{ur}^f + 2q_{tx}^2q_{1f}q_{ub}q_{ur}\left[P_{ur/\{1\}^b}^f\left(1 - P_{ur/\{1\}^f}^b\bar{P}_{ud/\{r\}^f}^b\right)\right. \\ & \left.+ \bar{P}_{ur/\{1\}^b}^fP_{ur/\{1\}^f}^b\bar{P}_{ud/\{r\}^f}^b + 2\left(P_{ur/\{1\}^f}^b\bar{P}_{ud/\{r\}^f}^b\right)^2\right] + 2q_{tx}^2q_{ub}q_{uf}q_{um}P_{ur}^b\bar{P}_{ud/\{1,r\}^f}^b + q_{tx}^2q_{ub}^2 \\ & \times \left[2P_{ur/\{1\}^b}^b\bar{P}_{ud/\{r\}^f,\{1\}^b}^b\left(1 - P_{ur/\{1\}^b}^b\bar{P}_{ud/\{r\}^f,\{1\}^b}^b\right) + 2\left(P_{ur/\{1\}^b}^b\bar{P}_{ud/\{r\}^f,\{1\}^b}^b\right)^2\right]. \end{aligned} \quad (6)$$

Therefore, the service rate is  $\mu_r = q_rB_r$ , where  $B_r$  can be expressed as follows:

$$\begin{aligned} B_r = & P_{rd}^f\left(\bar{q}_{tx}^2 + 2q_{tx}\bar{q}_{tx}q_{uf}q_{ur} + q_{tx}^2q_{uf}^2q_{2f}q_{ur}^2\right) + P_{rd/\{1\}^f}^f\left(2q_{tx}\bar{q}_{tx}q_{uf}q_{um} + 2q_{tx}^2q_{uf}^2q_{um}q_{ur}\right) \\ & + P_{rd/\{1\}^b}^f\left(2q_{tx}\bar{q}_{tx}q_{ub} + 2q_{tx}^2q_{ub}q_{uf}q_{ur} + P_{rd/\{2\}^f}^fq_{tx}^2q_{uf}^2q_{um}^2 + P_{rd/\{1\}^f,\{1\}^b}^f2q_{tx}q_{uf}q_{ub}q_{um}\right. \\ & \left.+ P_{rd/\{2\}^b}^fq_{tx}^2q_{ub}^2\right). \end{aligned} \quad (7)$$

By applying the Loyne's criterion [34], we can now obtain the range of values of  $q_r$  for which the queue is stable by solving the following inequality:  $\lambda_r^1 < \mu_r$ . Thus, we have that the queue at  $R$  is stable if and only if  $q_{rmin} < q_r \leq 1$ , where  $q_{rmin}$  is given by:

$$q_{rmin} = \frac{\lambda_r^0}{\lambda_r^0 + B_r - A_r}. \quad (8)$$

The evolution of the queue at the relay can be modelled as a discrete time Markov Chain (DTMC), as represented in Fig. 2. The terms  $p_k^0$  and  $p_k^1$  are the probabilities that the queue size

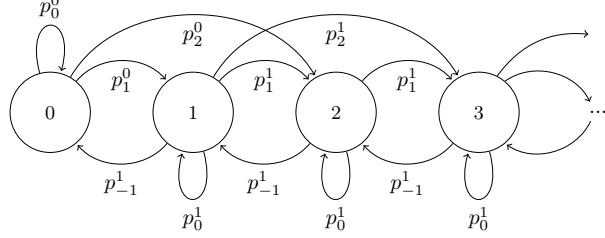


Fig. 2: The DTMC model for the two UE case.

increases by  $k$  packets in a timeslot when the queue is empty or not. These probabilities are derived in Appendix C. Moreover, the expressions for the probability that the queue is empty,  $P(Q = 0)$ , and the average relay queue size,  $\bar{Q}$ , are derived in Appendix D that contains the queue performance analysis for  $N$  symmetric UEs.

#### IV. THROUGHPUT AND DELAY ANALYSIS

##### A. Throughput Analysis

In this section, we derive the network aggregate throughput,  $T$ , for  $N$  UEs. When the queue at the relay  $R$  is stable,  $T$  can be expressed as follows:

$$T = Nq_{tx}T_u = Nq_{tx}q_{uf} \left( q_{um}T_{ud}^f + q_{ur}T_{ur}^f \right) + Nq_{tx}q_{ub} \left( T_{ud}^b + T_{ur}^b \right), \quad (9)$$

where,  $T_u$  is the per-user throughput conditioned to the event that the UE is transmitting. On the other hand, when the queue at  $R$  is unstable, the aggregate throughput becomes:

$$T = Nq_{tx} \left( q_{uf}q_{um}T_{ud}^f + q_{ub}T_{ud}^b \right) + \mu_r. \quad (10)$$

The terms,  $T_{ud}^f$ ,  $T_{ud}^b$ ,  $T_{ur}^f$ , and  $T_{ur}^b$  represent the contributions to  $T_u$  given by the packets received directly by the mmAP or by  $R$ , when the FD and the BR transmissions are used, respectively and can be expressed as follows:

$$T_{ud}^f = \left( 1 - q_r P(Q \neq 0) \right) T_{ud}^{f0} + q_r P(Q \neq 0) T_{ud}^{f1}, \quad (11)$$

$$T_{ud}^b = \left( 1 - q_r P(Q \neq 0) \right) T_{ud}^{b0} + q_r P(Q \neq 0) T_{ud}^{b1}, \quad (12)$$

$$T_{ur}^b = \left( 1 - q_r P(Q \neq 0) \right) T_{ur}^{b0} + q_r P(Q \neq 0) T_{ur}^{b1}, \quad (13)$$

where,  $P(Q = 0)$  is derived in Appendix D. Moreover, in (11), (12), and (13) we show the contributions to  $T_u$  (e.g.,  $T_{ud}^{f0}$  and  $T_{ud}^{f1}$ ) given by the packets that are sent to the mmAP or

both when  $R$  is interfering or not. These two cases are indicated with the superscripts 0 and 1, respectively. Note that the expression of  $T_{ur}^f$  is not affected by the interference of  $R$  because we assume perfect self-interference cancellation at the  $R$ . Hereafter, we indicate by  $m$  the number of UEs that interfere and with  $i$  the number of those that use FD transmissions ( $m - i$  UEs use the BR transmission). Moreover, among the interfering UEs that use FD transmissions, a certain number  $j$  transmit to  $R$  and  $i - j$  to the mmAP. Thus, we obtain the following:

$$T_{ud}^{f0} = \sum_{m=0}^{N-1} \binom{N-1}{m} q_{tx}^m \bar{q}_{tx}^{N-1-m} \sum_{i=0}^m \binom{m}{i} q_{uf}^i q_{ub}^{m-i} \sum_{j=0}^i \binom{i}{j} q_{ur}^j q_{um}^{i-j} P_{ud/\{i-j\}^f, \{m-i\}^b}^f, \quad (14)$$

$$T_{ud}^{b0} = \sum_{m=0}^{N-1} \binom{N-1}{m} q_{tx}^m \bar{q}_{tx}^{N-1-m} \sum_{i=0}^m \binom{m}{i} q_{uf}^i q_{ub}^{m-i} \sum_{j=0}^i \binom{i}{j} q_{ur}^j q_{um}^{i-j} \times P_{ud/\{i-j\}^f, \{m-i\}^b}^b, \quad (15)$$

$$T_{ud}^{f1} = \sum_{m=0}^{N-1} \binom{N-1}{m} q_{tx}^m \bar{q}_{tx}^{N-1-m} \sum_{i=0}^m \binom{m}{i} q_{uf}^i q_{ub}^{m-i} \sum_{j=0}^i \binom{i}{j} q_{ur}^j q_{um}^{i-j} P_{ud/\{i-j, r\}^f, \{m-i\}^b}^f, \quad (16)$$

$$T_{ud}^{b1} = \sum_{m=0}^{N-1} \binom{N-1}{m} q_{tx}^m \bar{q}_{tx}^{N-1-m} \sum_{i=0}^m \binom{m}{i} q_{uf}^i q_{ub}^{m-i} \sum_{j=0}^i \binom{i}{j} q_{ur}^j q_{um}^{i-j} P_{ud/\{i-j, r\}^f, \{m-i\}^b}^b. \quad (17)$$

Finally, we derive the terms  $T_{ur}^f$ ,  $T_{ur}^{b0}$  and  $T_{ur}^{b1}$  as follows:

$$T_{ur}^f = \sum_{m=0}^{N-1} \binom{N-1}{m} q_{tx}^m \bar{q}_{tx}^{N-1-m} \sum_{i=0}^m \binom{m}{i} q_{uf}^i q_{ub}^{m-i} \sum_{j=0}^i \binom{i}{j} q_{ur}^j q_{um}^{i-j} P_{ur/\{j\}^f, \{m-i\}^b}^f \quad (18)$$

$$T_{ur}^{b0} = \sum_{m=0}^{N-1} \binom{N-1}{m} q_{tx}^m \bar{q}_{tx}^{N-1-m} \sum_{i=0}^m \binom{m}{i} q_{uf}^i q_{ub}^{m-i} \sum_{j=0}^i \binom{i}{j} q_{ur}^j q_{um}^{i-j} P_{ur/\{j\}^f, \{m-i\}^b}^b \bar{P}_{ud/\{i-j\}^f, \{m-i\}^b}^b. \quad (19)$$

$$T_{ur}^{b1} = \sum_{m=0}^{N-1} \binom{N-1}{m} q_{tx}^m \bar{q}_{tx}^{N-1-m} \sum_{i=0}^m \binom{m}{i} q_{uf}^i q_{ub}^{m-i} \sum_{j=0}^i \binom{i}{j} q_{ur}^j q_{um}^{i-j} P_{ur/\{j\}^f, \{m-i\}^b}^b \bar{P}_{ud/\{i-j, r\}^f, \{m-i\}^b}^b. \quad (20)$$

## B. Delay Analysis

We now compute the average delay for a packet that is in the head of the queue of a UE. The delay is constituted of three components: i) the transmission delay (i.e., on the links UE-mmAP, UE-R, and R-mmAP), ii) the queueing delay at the relay  $D_q$ , and iii) the beam alignment phase

duration  $D_a$ . After a successful transmission, a new packet arrives at the head of the queue. At this point, as explained in Section II-A, the UE decides to transmit the packet with probability  $q_u$ .

Depending on the selected transmission strategies in the current timeslot and in the previous transmission attempt, the packet can be subject to different delays,  $D_i$  with  $i \in \mathcal{S}$ , where,  $\mathcal{S} = \{fm, fr, b\}$  and  $P(s = fm)$ ,  $P(s = fr)$ , and  $P(s = b)$  are defined in Section II-A. Given that the probability distributions of the transmission strategy selection  $P(s = i)$  are i.i.d. for each time slot, we can write the probability to use the  $i$ -th strategy in timeslot  $k$  – conditioned to using the  $j$ -th strategy in timeslot  $h$  – as follows:  $P(s_k = i \cap s_h = j) = P(s_k = i)P(s_h = j) = P(s = i)P(s = j)$ . Thus, we can express the average delay per packet as follows:

$$D = \sum_{i \in \mathcal{S}} P(s = i) \left( D_i + (1 - P(s = i))D_a \right), \quad (21)$$

Then, we compute the terms  $D_i$  of (21), which are given by:

$$\begin{aligned} D_{fm} &= q_u T_{ud}^f + q_u \left( 1 - T_{ud}^f \right) \left( 1 + q_{uf} q_{um} D_{fm} + q_{uf} q_{ur} (D_a + D_{fr}) + q_{ub} (D_a + D_b) \right) \\ &\quad + \bar{q}_u \left( 1 + D_{fm} \right), \end{aligned} \quad (22)$$

$$\begin{aligned} D_{fr} &= q_u T_{ur}^f (1 + D_r) + q_u \left( 1 - T_{ur}^f \right) \left( 1 + q_{uf} q_{ur} D_{fr} + q_{uf} q_{um} (D_a + D_{fm}) + q_{ub} (D_a + D_b) \right) \\ &\quad + \bar{q}_u \left( 1 + D_{fr} \right), \end{aligned} \quad (23)$$

$$\begin{aligned} D_b &= q_u T_{ud}^b + q_u T_{ur}^b (1 + D_r) + q_u \left( 1 - T_{ud}^b - T_{ur}^b \right) \\ &\quad \times \left( 1 + q_{ub} D_b + q_{uf} q_{um} (D_a + D_{fm}) + q_{uf} q_{ur} (D_a + D_{fr}) \right) + \bar{q}_u \left( 1 + D_b \right), \end{aligned} \quad (24)$$

where,  $T_{ud}^f$ ,  $T_{ud}^b$ ,  $T_{ur}^f$  and  $T_{ur}^b$  are several contributions to the conditioned per-user throughput  $T_u$  that are given in IV-A. Since a UE transmits at most one packet per timeslot,  $T_u$  can be also interpreted as the probability that a packet is successfully transmitted by a UE. The term  $D_r$  is the total delay at the relay that is defined as the time when the packet entering the relay queue reaches the mmAP and it is given by:

$$D_r = D_q + \frac{1}{\mu_r} = \frac{\bar{Q}}{\lambda_r} + \frac{1}{\mu_r}. \quad (25)$$

where,  $D_q$  in (25) is the queueing delay at the relay. The latter is the time when the packet being received by the relay reaches the head of its queue and it is computed by using the Little's law. More precisely,  $\bar{Q}$  represents the average relay queue size and  $\lambda_r$  the average arrival rate,

which are given in Appendix D. Finally, by considering (25) and replacing (22), (23), and (24) in (21), the average delay per packet  $D$  can be written as follows:

$$D = \frac{1 + q_u D_r \left( q_{uf} q_{ur} T_{ur}^f + q_{ub} T_{ur}^b \right) + D_a q_u C}{q_u T_u}, \quad (26)$$

where,  $C$  is given by:

$$C = 1 + q_{uf}^2 q_{um}^2 \left( T_{ud}^f - T_u - 1 \right) + q_{uf}^2 q_{ur}^2 \left( T_{ur}^f - T_u - 1 \right) + q_{ub}^2 \left( T_{ud}^b + T_{ur}^b - T_u - 1 \right). \quad (27)$$

## V. NUMERICAL & SIMULATION RESULTS

In this section, we provide a numerical evaluation of the performance analysis derived for throughput and delay. Furthermore, we assess the validity of the analysis by comparing the numerical results of the analytical model with simulations. In order to compute the LOS and NLOS probabilities and the path loss, we use the 3GPP model for urban micro cells in outdoor street canyon environment [35]. More precisely, the path loss depends on the height of the mmAP, 10 m, the height of the UE, 1.5 m, the carrier frequency,  $f_c = 30$  GHz, and the distance between the transmitter and the receiver. The transmit power and the noise power are set to  $P_t = 24$  dBm and  $P_N = -80$  dBm, respectively. Then, the SINR in (1) and the success probability in (28) are numerically computed by considering 100,000 instances of the lognormal shadowing. This success probability represents the input for both the numerical evaluations of the analytical model and simulations results, which are computed over 100,000 timeslots. Moreover, unless otherwise specified, we set  $d_{ur} = 30$  m,  $d_{ud} = 50$  m,  $\gamma = 10$  dB,  $\alpha = 0.1$  and, in case of FD transmissions,  $\theta_{BW} = 5^\circ$ . Instead, when a BR transmission is used, we set  $\theta_{BW} = \theta_{rd}$ , which is the angle between the mmAP and  $R$  with the UE as vertex. Throughout this section, we use solid lines for numerical evaluations of the analytical model and dotted lines for the simulation results.

In Fig. 3a and Fig. 3b, we show the throughput,  $T$ , while varying the number of UEs ( $N$ ) for several UE transmit probability values, i.e.,  $q_u$ , when  $D_a = 0$  and  $D_a = 5$ , respectively. For both the cases, we can observe that the analytical model and the simulations almost coincide. Furthermore, in Fig. 3a, we can observe that for  $q_u = 0.1$  the throughput is an increasing function of  $N$  and the queue at  $R$  is always stable. In contrast, for  $q_u = 0.5$  and  $q_u = 0.9$  the queue becomes unstable at  $N = 6$  and  $N = 3$ , respectively, which is also approximately the point at which  $T$  reaches its the maximum. After this point, increasing  $N$  causes a decrease of the throughput. Namely, high values of  $N$  and  $q_u$  lead to high interference that decreases the number

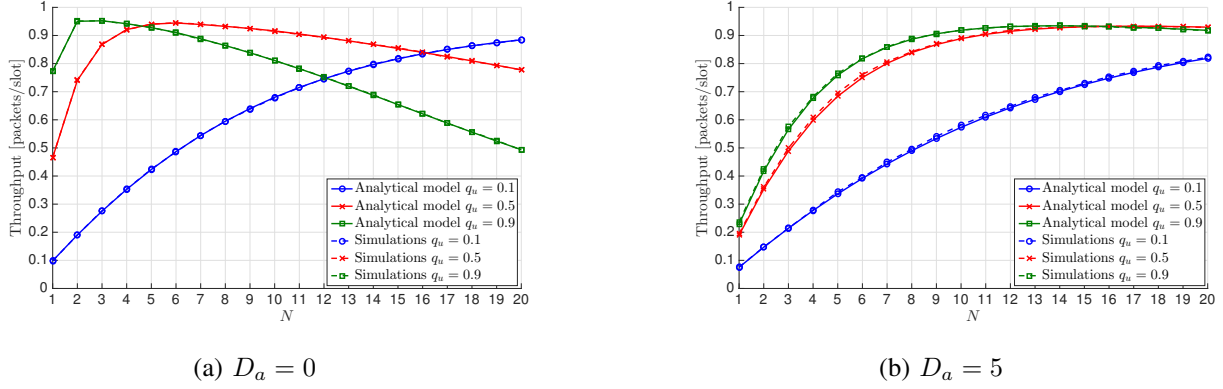


Fig. 3: Throughput,  $T$ , while varying the number of UEs for several UE transmit probability values, i.e.,  $q_u$ , when a)  $D_a = 0$  and b)  $D_a = 5$ , respectively.

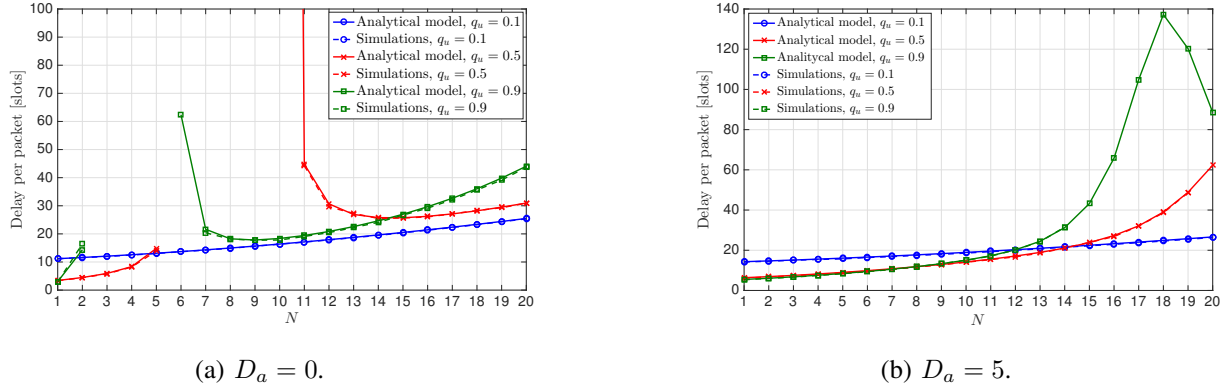


Fig. 4: Delay per packet,  $D$ , while varying the number of UEs for several UE transmit probability values, i.e.,  $q_u$ , when a)  $D_a = 0$  and b)  $D_a = 5$ , respectively.

of packets successfully received by  $R$  and the mmAP. As a consequence, the decreasing number of arrivals makes the queue at the relay again stable. For  $q_u = 0.5$  and  $q_u = 0.9$  the queue becomes stable at  $N = 10$  and  $N = 7$ , respectively. In Fig. 3b, the larger value of the beam alignment delay,  $D_a = 5$ , decreases the transmit probability. The queue is always stable for the considered values of  $q_u$ . Moreover, the maximum value of the throughput is lower with respect to the one in Fig. 3a.

The stability and instability regions can be better observed in Fig. 4a and Fig. 4b, which show the results for the analytical model and the simulations for the delay, when assuming the same system parameters of Fig. 3a and Fig. 3b, respectively. In Fig. 4a, we can identify three regions, corresponding to the cases for which the queue at the relay is stable ( $\lambda_r < \mu_r$ ), unstable

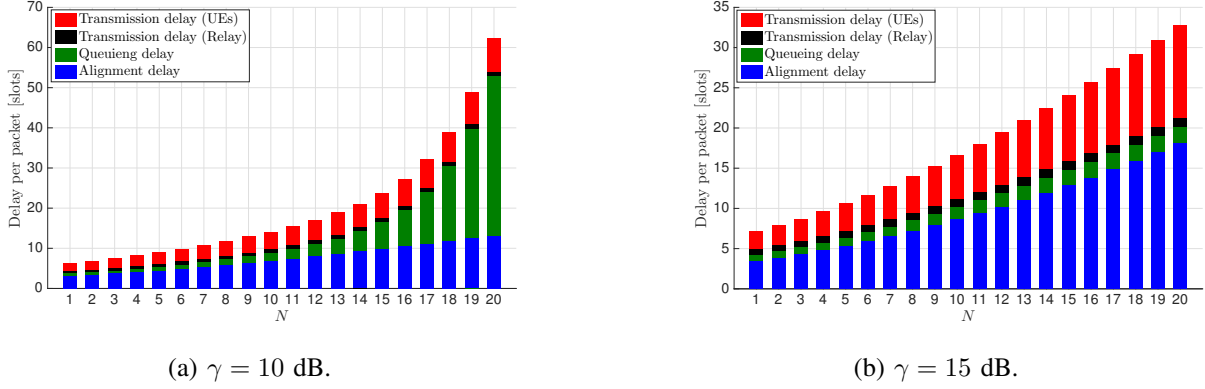


Fig. 5: Delay per packet while varying the number of UEs,  $N$ , with  $q_u = 0.5$  and  $D_a = 5$ .

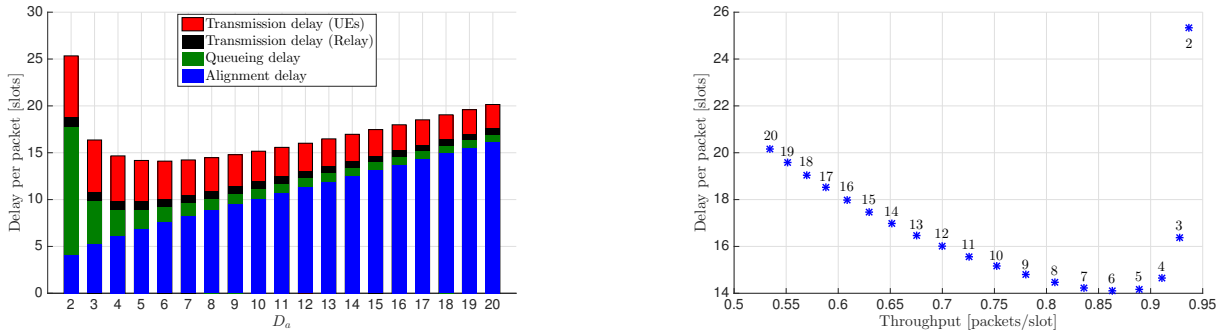


Fig. 6: Delay per packet while varying the beam alignment duration,  $D_a$ , with  $q_u = 0.5$  and  $N_a = 10$ .

Fig. 7: Throughput vs. delay tradeoff for several values of  $D_a$ , with  $q_u = 0.5$  and  $N_a = 10$ . For each point we report the corresponding value of  $D_a$ .

$(\lambda_r > \mu_r)$  and instable  $(\lambda_r = \mu_r)$ . In this latest case, the arrival rate  $\lambda_r$  is still below the service rate  $\mu_r$ , but very close to it. The three regions can be easily distinguished in the figures, since for the case of instable queue we report only the analytical results (since simulation results are meaningless), for the unstable queue we do not report any results, because the delay increases towards infinity, and only for the stable case we report both analytical and simulation results. For  $q_u = 0.1$ , there is neither instability nor instability regions. In contrast, the region for which the queue is instable,  $\lambda_r \approx \mu_r$ , can be clearly observed for  $q_u = 0.5$  ( $N = 10$ ) and  $q_u = 0.9$  ( $N = 6$ ), where the delay values is still finite, but very high.

The transmit probability  $q_{tx}$  and the arrival packet rate at the relay decrease by increasing the value of the beam alignment delay to  $D_a = 5$ . The effects of this can be observed in Fig. 4b, where the queue is never unstable and the instability regions change as well. Namely,

the instability region for  $q_u = 0.5$  is visible at  $N = 20$ , whereas, for  $q_u = 0.9$  it is between  $N = 15$  and  $N = 20$ . For regions far from instability, the analytical model and the simulations almost coincide and the delay increases with the increasing number of UEs for all the curves.

The increasing trend of the delay is caused by two main reasons: i) an increasing number of packets inside the queue and ii) increasing interference (that reduces the success probability of transmission). For a better understanding of this phenomenon, we show in Fig. 5a the delay per packet as sum of its components, i.e., UE's and relay transmission delays and queueing and alignment delays, for the red curve shown in Fig. 4b ( $q_u = 0.5$ ,  $D_a = 5$ , and  $\gamma = 10$  dB). We can observe that close to the instability region ( $N = 20$ ) the biggest delay component is given by the queueing delay, whereas the transmission delays (both UE and  $R$ ) as well as the alignment delay are barely increasing with  $N$ . A different behavior can be observed in Fig. 5b, where the same scenario of Fig. 5a is considered but for a higher SINR threshold, i.e.,  $\gamma = 15$  dB. In this case, the higher value of  $\gamma$  reduces the success probability of transmission and the arrivals at the relay. Thus, the queueing delay does not represent anymore the main issue, nor does the relay transmission delay. In contrast, the increased unsuccessful transmission attempts make the packets waiting for being transmitted for most of the time inside the UEs' queue that increases the UE transmission and the alignment delays. This is also due to the fact that, as explained in Section II, after a transmission attempt the UE can change transmission strategy.

In Fig. 6, we show the impact of the beam alignment duration  $D_a$  on the delay components. We set the number of UEs  $N = 10$ ,  $q_u = 0.5$ , and  $\gamma = 10$  dB while increasing the value of  $D_a$ . First, we can observe that the delay has a non-monotonic behavior. More precisely, for  $D_a = 0$  and  $D_a = 1$  the queue is instable and unstable, respectively, and we do not report any value. Then, the delay decreases at first, mostly because the increased  $D_a$  reduces the transmit probability and the arrival rate at the relay queue. This is confirmed by the decrease in the queueing delay that represents the highest delay component for lower values of  $D_a$ . However, above a certain value of  $D_a$ , the delay start increasing again mostly because the alignment delay increases. In contrast to the delay, the throughput has a slightly different behavior. In Fig. 7, we show the throughput and delay tradeoff for several values of  $D_a$  and it can be observed that the throughput monotonically decreases.

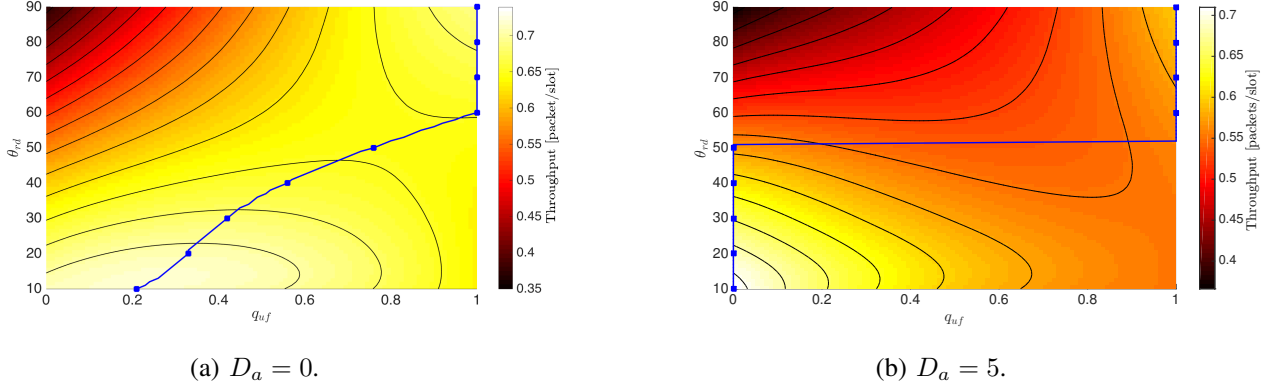


Fig. 8: Throughput,  $T$ , while varying  $q_{uf}$  and  $\theta_{rd}$ , with  $q_{ur} = 0.5$ . For each value of  $\theta_{rd}$ , we represent with a blue solid line the value of  $q_{uf}$  that maximizes the throughput.

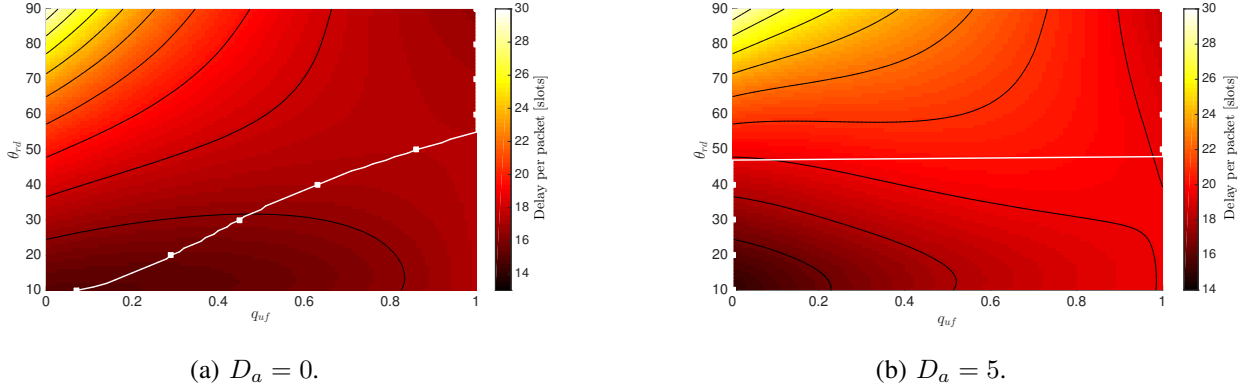


Fig. 9: Delay per packet,  $D$ , while varying  $q_{uf}$  and  $\theta_{rd}$ , with  $q_{ur} = 0.5$ . For each value of  $\theta_{rd}$ , we represent with a white solid line the value of  $q_{uf}$  that minimizes the delay.

### A. Optimal Transmission Strategy

Hereafter, we set  $q_u = 0.1$  and  $N = 10$  (i.e. the queue is always stable) and we study the effect of the two transmission strategies (FD and BR) on the throughput and the delay. In Fig. 8a, we set  $q_{ur} = 0.5$  and show the aggregate throughput,  $T$ , while varying the probability of using the FD transmission,  $q_{uf}$ , and  $\theta_{rd}$ , for  $D_a = 0$ . The solid blue line shows the values of  $q_{uf}$  that maximizes the throughput for each value of  $\theta_{rd}$ . Namely, for small values of  $\theta_{rd}$ , the BR transmission is preferable (corresponding to small values of  $q_{uf}$ ). In this case, we can use a narrow beam with high beamforming gain to transmit simultaneously to  $R$  and the mmAP. In contrast, for higher values of  $\theta_{rd}$ , the optimal value of  $q_{uf}$  becomes 1, which corresponds to using

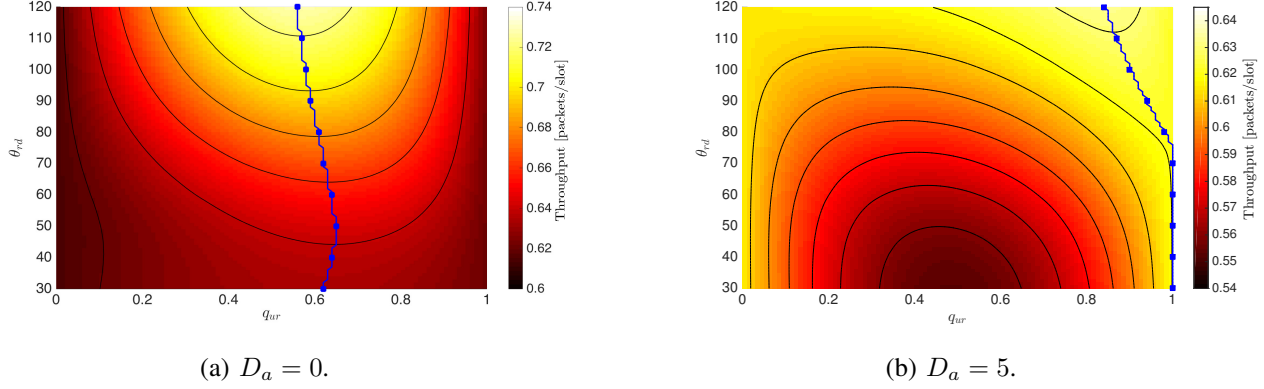


Fig. 10: Throughput,  $T$ , while varying  $q_{ur}$  and  $\theta_{rd}$  with  $q_{uf} = 1$ . For each value of  $\theta_{rd}$ , we represent with a solid blue line the value of  $q_{ur}$  that maximizes the throughput.

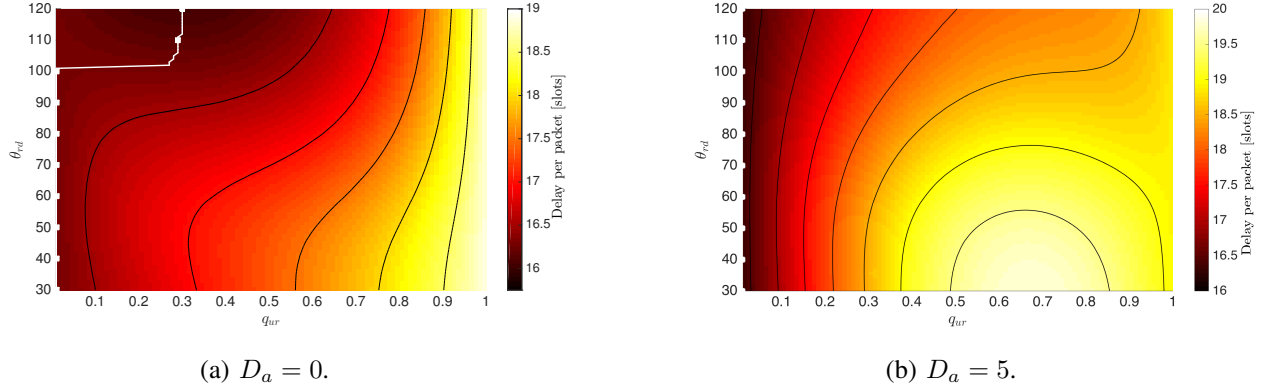


Fig. 11: Delay per packet,  $D$ , while varying  $q_{ur}$  and  $\theta_{rd}$ , with  $q_{uf} = 1$ . For each value of  $\theta_{rd}$ , we represent with a white solid line the value of  $q_{ur}$  that minimizes the delay.

the FD transmission. For  $D_a = 5$ , in Fig. 8b, we have almost the same behavior. However, the selection of the best strategy is either  $q_{uf} = 0$  or  $q_{uf} = 1$ , since the number of beam alignments is minimized and  $q_{tx}$  maximized when  $q_{uf} = 0$  or  $q_{uf} = 1$ .

In Fig. 9a and Fig. 9b we show the delay for the same setting of Fig. 8a and Fig. 8b, respectively, while varying  $q_{uf}$ , and  $\theta_{rd}$ . For this scenario, where the queue is stable, the highest contributions to the delay are given by the transmission and alignment delays. For this reason the strategy that minimizes the delay, which is shown with a white solid line, follows almost the same behavior of the transmission strategy that maximizes the throughput.

In Fig. 10, we show the throughput  $T$  while varying the probability to transmit at the relay  $q_{ur}$  and  $\theta_{rd}$ , when the FD transmission is used, i.e.,  $q_{uf} = 1$ . Note that larger values of  $\theta_{rd}$

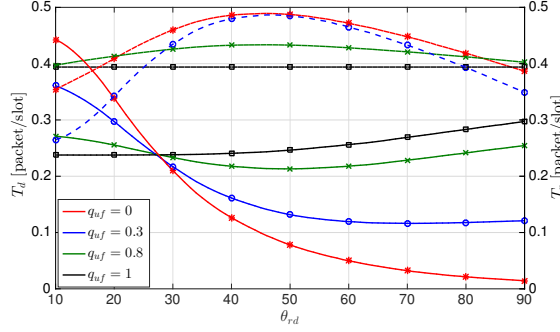


Fig. 12:  $T_d$  (solid lines) and  $T_r$  (dotted lines) with varying  $\theta_{rd}$  for several values of  $q_{uf}$ , with  $q_{ur} = 0.5$  and  $D_a = 0$ .

correspond to longer distances between  $R$  and the mmAP, i.e.,  $d_{rd}$  (see Fig. 1). Thus, when  $\theta_{rd}$  increases, the interference of the relay on the transmission to the mmAP decreases. As explained in Section II, the relay is in LOS with the mmAP and uses always the FD transmission with high beamforming gain. Such high gain can cause high interference at the receiver side of the mmAP. As results of this, we can observe higher throughput for larger values of  $\theta_{rd}$ . This phenomenon is better explained in the following. In Fig. 10a, for which  $D_a = 0$ , the strategy that maximizes  $T$  is shown by a solid blue line and is  $q_{ur} \approx 0.6$  for all the values of  $\theta_{rd}$ . In contrast, in Fig. 10b, where  $D_a = 5$ , we observe a different behavior. The optimal strategy coincides with  $q_{ur} = 1$  for lower value of  $\theta_{rd}$  that allows to minimize the probability to change strategy. When  $\theta_{rd}$  increases, the highest throughput is provided by a slightly smaller value of  $q_{ur}$ , with an increase in the transmissions to the mmAP.

For the same settings of Fig. 10a and Fig. 10b, we show the results for delay in Fig. 11a and Fig. 11b, respectively. First, we can observe that the best transmission strategy for the delay is different from the one for the throughput. Indeed, for the throughput it is more beneficial to transmit to the relay  $R$ , while it is preferable to transmit to the mmAP for minimizing the delay. Namely, by transmitting to the mmAP the packets avoid the queueing delay at the relay and the interference that this creates on the mmAP, since the relay transmits a lower amount of packets.

In Fig. 10a and Fig. 10b, we observe that for the FD transmission and short distances ( $d_{ur} = 30$  m and  $d_{ud} = 50$  m), we have higher values of  $T$  as  $\theta_{rd}$  increases. This can be better explained in Fig. 12, which shows the aggregate throughput when directly transmitted to the mmAP and when using  $R$ , i.e.,  $T_d$  and  $T_r$ , respectively, while varying  $\theta_{rd}$  for several values of  $q_{uf}$ . We set

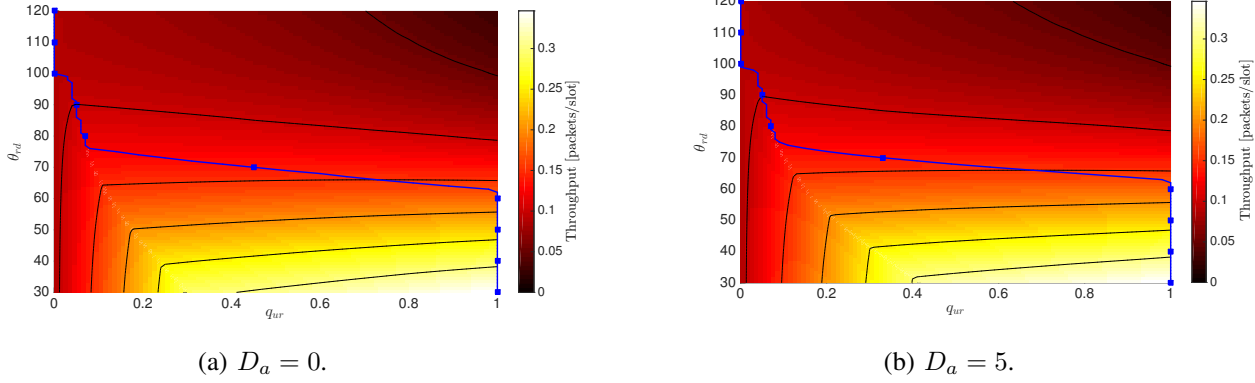


Fig. 13: Throughput,  $T$ , while varying  $q_{ur}$  and  $\theta_{rd}$  with  $q_{uf} = 1$ ,  $d_{ur} = 30$  m and  $d_{ud} = 50$  m. For each value of  $\theta_{rd}$ , we represent with a solid blue line the value of  $q_{ur}$  that maximizes the throughput.

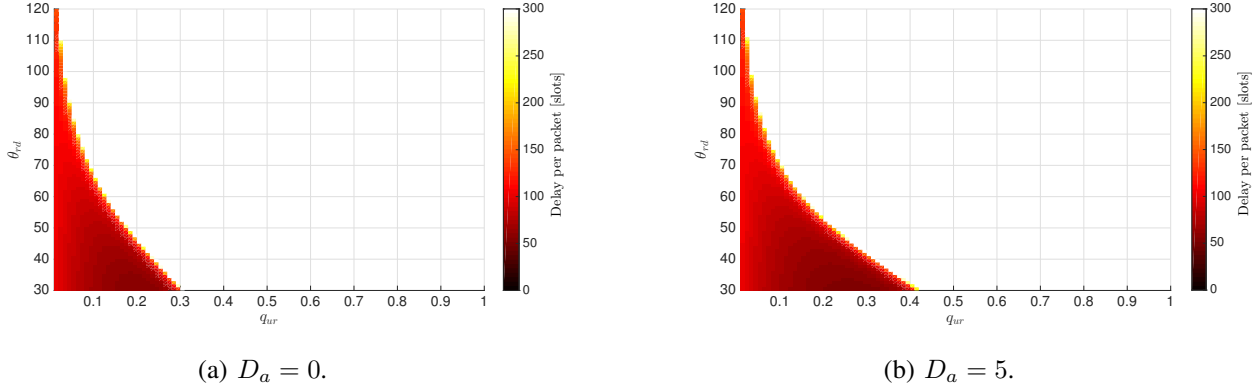


Fig. 14: Delay per packet,  $D$ , while varying  $q_{ur}$  and  $\theta_{rd}$ , with  $q_{uf} = 1$ ,  $d_{ur} = 30$  m and  $d_{ud} = 50$  m.

$D_a = 0$ , but the results are valid also for higher values of the beam alignment delay. Since the  $R$ -mmAP link is always in LOS, the success probability for a packet transmitted from  $R$  to the mmAP, hence  $T_r$  (dotted lines), is barely affected by increasing the distance between  $R$  and the mmAP. In contrast,  $T_d$  (solid lines) increases for wider  $\theta_{rd}$  because the interference caused by  $R$  decreases. For  $0 < q_{uf} < 1$ ,  $T_d$  and  $T_r$  have a non-monotonic behavior. When  $\theta_{rd}$  increases initially,  $T_d$  decreases because of two reasons. First, the beamforming gain of the BR transmissions decreases, and so the probability for sending a packet successfully by using the BR transmission. At the same time, the packets that are not successfully received by the mmAP may be stored in the queue at  $R$ . The increase in the stored packets by  $R$  corresponds to an increase in the interference at the receiver side of the mmAP that is caused by the relay.

In turn, the increase in the interference represents the second reason for the decrease of  $T_d$ . We can observe that  $T_r$  increases at the beginning. However, when  $\theta_{rd}$  exceeds a certain threshold,  $T_r$  starts decreasing because wider beams with lower beamforming gains are not enough to overcome the path loss.

Finally, we show the effects of increasing the distances, i.e.,  $d_{ud}$  and  $d_{ur}$ , when considering the same scenario of Fig. 10. In Fig. 13a, we show the throughput with longer distances i.e.,  $d_{ur} = 50$  m,  $d_{ud} = 200$  m, and  $D_a = 0$ . The blue solid line shows the transmission strategy for maximizing the throughput. We can observe that for lower values of  $\theta_{rd}$  the transmissions to the relay are preferable, as in Fig. 10a. However, for longer distances  $d_{rd}$  (high values of  $\theta_{rd}$ ), the relay does not become anymore beneficial and in general  $T$  decreases. As a result, the transmissions between the UEs and the mmAP are barely affected by the interference of  $R$  and the link path loss between  $R$  and the mmAP is dominant. This link path loss decreases the success probability for a packet sent from  $R$  to the mmAP and makes the queue at  $R$  not stable when  $q_{ur}$  is above certain values. The unstability and instability regions can be better observed in Fig. 14a, where we show the delay for  $D_a = 0$ . Here, we do not report (i.e. white area) the values of  $q_{ur}$  and  $\theta_{rd}$  for which the queue is unstable. For higher value of  $D_a$ , we can observe in Fig 14a and Fig 14b that the instability region changes, but the optimal strategy for the throughput have almost the same behavior.

## VI. CONCLUSION

In this work, we presented a throughput and delay analysis for relay assisted mm-wave wireless networks, where the UEs can transmit by using either an FD or a BR transmission. In particular, we analyzed the performance of the queue at the relay by deriving the stability conditions as well as the arrival and service rates. We numerically evaluated the analytical model and validated our analysis with simulations.

The analytical model matches well the simulation results. The latter show that beam alignment causes a decrease in the transmit probability inversely proportional to the beam alignment duration,  $D_a$ , and the probability to change the strategy. We have shown how, in case of queue stability, the increase in  $D_a$  decreases the throughput and the delay. However, for dense scenarios, where the queue at the relay is close to becoming unstable, the increase in  $D_a$  can decrease the delay per packet. More precisely, when being close to the instability condition, we could show

that the highest delay component is given by the queueing delay. Whereas, when the queue is stable, the delay is affected mostly by the transmission and alignment delay.

Moreover, we showed that the optimal transmission strategy highly depends on the network topology, e.g.,  $d_{ud}$ ,  $d_{ur}$ ,  $\theta_{rd}$ , and the queue condition. When the queue is stable, the values of  $q_{uf}$  and  $q_{ur}$  that maximize the throughput and minimize the delay usually coincide. However, when being close to the instability and instability regions, the throughput and delay present a tradeoff. Furthermore, as expected, we showed that is not always beneficial to use narrow beams (FD) compared to wider beams (BR). As a matter of fact, for short distances and a beamwidth of  $30^\circ$ , a broadcast transmission is still preferable, although it provides a lower beamforming gain than FD. When the distances or the SINR threshold increase, an FD strategy should be chosen.

Finally, we could observe, that for the evaluated scenarios, the interference caused by the relay and the link path loss represent the main impediments for the success probability, hence the throughput and the delay, in case of short and long distances among the nodes, respectively.

## APPENDIX A

We now derive the success probability expression, conditioned to the sets  $\mathcal{I}_f$  and  $\mathcal{I}_b$ , for a generic link  $ij$  with  $N$  symmetric UEs. In order to average on all the possible scenarios for the LOS and NLOS links, we consider that  $k$  and  $h$  UEs over  $|\mathcal{I}_f|$  and  $|\mathcal{I}_b|$  interferers, respectively, are in LOS. Thus, the success probability can be derived as follows:

$$\begin{aligned}
P_{ij/\mathcal{I}_f, \mathcal{I}_b}^f &= P(\text{LOS}_{ij})P(\text{SINR}_{ij/\mathcal{I}_f, \mathcal{I}_b}^f \geq \gamma | \text{LOS}_{ij}) + P(\text{NLOS}_{ij})P(\text{SINR}_{ij/\mathcal{I}_f, \mathcal{I}_b}^f \geq \gamma | \text{NLOS}_{ij}) \\
&= P(\text{LOS}_{ij}) \left[ \sum_{k=0}^{|\mathcal{I}_f|} \binom{|\mathcal{I}_f|}{k} P(\text{LOS}_{ij})^k P(\text{NLOS}_{ij})^{|\mathcal{I}_f|-k} \sum_{h=0}^{|\mathcal{I}_b|} \binom{|\mathcal{I}_b|}{h} P(\text{LOS}_{ij})^h P(\text{NLOS}_{ij})^{|\mathcal{I}_b|-h} \right. \\
&\quad \times P(\text{SINR}_{ij/\mathcal{I}_{fl}, \mathcal{I}_{fn}, \mathcal{I}_{bl}, \mathcal{I}_{bn}}^f \geq \gamma | \text{LOS}_{ij}) \Big] + P(\text{NLOS}_{ij}) \left[ \sum_{k=0}^{|\mathcal{I}_f|} \binom{|\mathcal{I}_f|}{k} P(\text{LOS}_{ij})^k P(\text{NLOS}_{ij})^{|\mathcal{I}_f|-k} \right. \\
&\quad \times \left. \sum_{h=0}^{|\mathcal{I}_b|} \binom{|\mathcal{I}_b|}{h} P(\text{LOS}_{ij})^h P(\text{NLOS}_{ij})^{|\mathcal{I}_b|-h} P(\text{SINR}_{ij/\mathcal{I}_{fl}, \mathcal{I}_{fn}, \mathcal{I}_{bl}, \mathcal{I}_{bn}}^f \geq \gamma | \text{NLOS}_{ij}) \right], \tag{28}
\end{aligned}$$

where,  $P(\text{SINR}_{ij/\mathcal{I}_f, \mathcal{I}_b}^f \geq \gamma | \text{LOS}_{ij})$  and  $P(\text{SINR}_{ij/\mathcal{I}_f, \mathcal{I}_b}^f \geq \gamma | \text{NLOS}_{ij})$  are the probabilities that the received SINR is above  $\gamma$ , when link  $ij$  is in LOS and NLOS, respectively, conditioned to the specific scenarios of interferers,  $\mathcal{I}_f$  and  $\mathcal{I}_b$ . Whereas, the expression for  $P(\text{SINR}_{ij/\mathcal{I}_{fl}, \mathcal{I}_{fn}, \mathcal{I}_{bl}, \mathcal{I}_{bn}}^f \geq \gamma | \text{LOS}_{ij})$  is given in (1).

## APPENDIX B

In this appendix, we provide the proof of Theorem 1.

*Proof.* In order to compute the probability that a UE transmits in timeslot  $k$ , we identify the following mutual exclusive events:

- 1) the UE is performing a beam alignment. In this case the UE can not transmit and we have that  $q_{tx} = 0$ .
- 2)  $Al_{k-D_a}$ : the UE starts a beam alignment in timeslot  $k - D_a$ . In this case  $q_{tx} = 1$ . This is because the UE may start a beam alignment only if it decides to transmit.
- 3)  $I_k$ : the UE has not started an alignment in the previous  $D_a$  timeslots with respect to the  $k$ -th timeslot ( $k - D_a, k - D_a - 1, \dots, k - 1$ ). In this case, the UE can transmit in timeslot  $k$ , if and only if it decides to transmit with the same strategy used in the previous transmission attempt. Thus,  $q_{tx} = q_u P(s_k = i \cap s_{\hat{k}} = i)$ , with,  $i \in \mathcal{S}$ , and  $\hat{k}$  represents the timeslot where the previous transmission attempt occurs with respect to the  $k$ -th timeslot.

First, we analyze the second event. This occurs when in timeslot  $k - D_a$  the following two independent events hold: i)  $I_{k-D_a}$  and ii) *the UE decides to transmit with a different strategy with respect to the one that is used in the previous transmission attempt*. Therefore, the event  $Al_{k-D_a}$  occurs with probability:

$$P(Al_{k-D_a}) = P(I_{k-D_a})q_u(1 - P(s_{k-D_a} = i \cap s_{\hat{k}} = i)) \quad (29)$$

Thus, we can express  $q_{tx}$  as follows:

$$\begin{aligned} q_{tx} &= P(Al_{k-D_a}) + P(I_k)q_u P(s_k = i \cap s_{\hat{k}} = i) \\ &= P(I_{k-D_a})q_u(1 - P(s_{k-D_a} = i \cap s_{\hat{k}} = i)) + P(I_k)q_u P(s_k = i \cap s_{\hat{k}} = i) \\ &= P(I_k)q_u, \end{aligned} \quad (30)$$

where, in the first equality we exploit the mutual exclusivity of the three above-mentioned events. In the second equality of (30), we take into account (29) and in the last equality we have assumed that  $P(s_k = i)$  is i.d. for each timeslot  $k$ , which leads to the following:  $P(I_{k-D_a}) = P(I_k)$  and  $P(s_{k-D_a} = i \cap s_{\hat{k}} = i) = P(s_k = i \cap s_{\hat{k}} = i)$ .

Let us evaluate the probability of the complementary event of  $I_k$ , i.e.,  $\bar{I}_k$ . This event occurs when the UE starts a beam alignment in one of timeslots  $k - D_a, k - D_a - 1, \dots, k - 1$ . Thus,

$P(\bar{I}_k)$  is derived as the probability of the union of the following mutually exclusive events:  $\bigcup_{i=k-D_a}^{k-1} Al_i$ :

$$\begin{aligned}
P(\bar{I}_k) &= P\left(\bigcup_{i=k-D_a}^{k-1} Al_i\right) = \sum_{i=k-D_a}^{k-1} P(Al_i) \\
&= \sum_{i=k-D_a}^{k-1} P(I_i) q_u (1 - P(s_i = j \cap s_{\bar{i}} = j)) \\
&= D_a P(I_k) q_u (1 - P(s_k = i \cap s_{\bar{k}} = i)),
\end{aligned} \tag{31}$$

where, in the last step of (31), we use the same reasoning for the last equality of (30). Finally, by replacing (31) in  $P(\bar{I}_k) = 1 - P(I_k)$  we obtain (2).  $\square$

## APPENDIX C

In this appendix, we provide the transition probabilities  $p_k^0$  and  $p_k^1$  for the two UE case.

$$\begin{aligned}
p_{-1}^1 &= q_r \left[ P_{rd}^f \left( \bar{q}_{tx}^2 + 2q_{tx}\bar{q}_{tx}q_{uf}q_{ur}\bar{P}_{ur}^f + (q_{tx}q_{uf}q_{ur}\bar{P}_{ur/\{1\}^f}^f)^2 \right) + P_{rd/\{1\}^f}^f \right. \\
&\quad \times \left( 2q_{tx}\bar{q}_{tx}q_{uf}q_{um} + 2q_{tx}^2q_{uf}^2q_{um}q_{ur}\bar{P}_{ur}^f \right) + P_{rd/\{1\}^b}^f \left( 2q_{tx}\bar{q}_{tx}q_{ub}(1 - P_{ur}^b\bar{P}_{ud/\{r\}^f}^b) \right. \\
&\quad + 2q_{tx}^2q_{ub}q_{uf}q_{ur}(1 - P_{ur/\{1\}^f}^b\bar{P}_{ud/\{r\}^f}^b)\bar{P}_{ur/\{1\}^b}^f \left. \right) + P_{rd/\{1\}^f,\{1\}^b}^f 2q_{tx}^2q_{uf}q_{ub}q_{um}(1 - P_{ur}^b\bar{P}_{ud/\{1,r\}^f}^b) \\
&\quad \left. + P_{rd/\{2\}^b}^f \left( q_{tx}q_{ub}(1 - P_{ur/\{1\}^b}^b\bar{P}_{ud/\{r\}^f,\{1\}^b}^b) \right)^2 \right] + P_{rd/\{2\}^f}^f q_{tx}^2q_{uf}^2q_{um}^2.
\end{aligned} \tag{32}$$

$$\begin{aligned}
p_1^0 &= 2q_{tx}\bar{q}_{tx}q_{uf}q_{ur}P_{ur}^f + 2q_{tx}\bar{q}_{tx}q_{ub}P_{ur}^b\bar{P}_{ud}^b + 2q_{tx}^2q_{uf}^2q_{ur}^2P_{ur/\{1\}^f}^f\bar{P}_{ur/\{1\}^f}^f + 2q_{tx}^2q_{uf}^2q_{ur}q_{um}P_{ur}^f \\
&\quad + 2q_{tx}^2q_{uf}q_{ub}q_{ur} \left[ P_{ur/\{1\}^b}^f \left( 1 - P_{ur/\{1\}^f}^b\bar{P}_{ud}^b \right) + \bar{P}_{ur/\{1\}^b}^f P_{ur/\{1\}^f}^b\bar{P}_{ud}^b \right] + 2q_{tx}^2q_{ub}q_{uf}q_{um}P_{ur}^b\bar{P}_{ud/\{1\}^f}^b \\
&\quad + q_{tx}^2q_{ub}^2 \left[ 2P_{ur/\{1\}^b}^b\bar{P}_{ud/\{1\}^b}^b \left( 1 - P_{ur/\{1\}^b}^b\bar{P}_{ud/\{1\}^b}^b \right) \right].
\end{aligned} \tag{33}$$

$$\begin{aligned}
p_1^1 &= \bar{q}_r p_1^0 + q_r \left[ 2q_{tx}\bar{q}_{tx}q_{uf}q_{ur}P_{ur}^f\bar{P}_{rd}^f + 2q_{tx}\bar{q}_{tx}q_{ub}P_{ur}^b\bar{P}_{ud/\{r\}^f}^b\bar{P}_{rd/\{1\}^b}^f \right. \\
&\quad + 2q_{tx}^2q_{uf}^2q_{um}q_{ur}P_{ur}^f\bar{P}_{rd/\{1\}^f}^f + 2q_{tx}^2q_{uf}q_{ub}q_{um}P_{ur}^b\bar{P}_{ud/\{1,r\}^f}^b\bar{P}_{rd/\{1\}^f,\{1\}^b}^f \\
&\quad + q_{tx}^2q_{uf}^2q_{ur}^2 \left( P_{ur/\{1\}^f}^f\bar{P}_{ur/\{1\}^f}^f\bar{P}_{rd}^f + (P_{ur/\{1\}^f}^f)^2P_{rd}^f \right) + q_{tx}^2q_{ub}^2 \left( 2P_{ur/\{1\}^b}^b\bar{P}_{ud/\{r\},\{1\}}^b\bar{P}_{rd/\{2\}^b}^f \right. \\
&\quad \times \left. (1 - P_{ur/\{1\}^b}^b\bar{P}_{ud/\{r\}^f,\{1\}^b}^b) + (P_{ur/\{1\}^b}^b\bar{P}_{ud/\{r\}^f,\{1\}^b}^b)^2P_{rd/\{2\}^b}^f \right) \\
&\quad + 2q_{tx}^2q_{ub}q_{uf}q_{ur} \left( P_{ur/\{1\}^f}^b\bar{P}_{ud/\{r\}^f}^b\bar{P}_{ur/\{r\}^f,\{1\}^b}^b\bar{P}_{rd/\{1\}^b}^f + (1 - P_{ur/\{1\}^f}^b\bar{P}_{ud/\{r\}^f}^b)P_{ur/\{1\}^b}^f\bar{P}_{rd/\{1\}^b}^f \right. \\
&\quad \left. + P_{ur/\{2\}^f}^b\bar{P}_{ud/\{r\}^f}^bP_{ur/\{1\}^b}^fP_{rd/\{1\}^b}^f \right].
\end{aligned} \tag{34}$$

$$p_2^0 = \left( q_{tx} q_{uf} q_{ur} P_{ur/\{1\}^f}^f \right)^2 + \left( q_{tx} q_{ub} P_{ur/\{1\}^b}^b \bar{P}_{ud/\{r\}^f, \{1\}^b}^b \right)^2 + 2 q_{tx}^2 q_{ub} q_{uf} q_{ur} P_{ur/\{1\}^f}^b \bar{P}_{ud}^b P_{ur/\{1\}^b}^f. \quad (35)$$

$$p_2^1 = \bar{q}_r p_2^0 + q_r \left[ \left( q_{tx} q_{uf} q_{ur} P_{ur/\{1\}^f}^f \right)^2 \bar{P}_{rd}^f + \left( q_{tx} q_{ub} P_{ur/\{1\}^b}^b \bar{P}_{ud/\{r\}^f, \{1\}^b}^b \right)^2 \bar{P}_{rd/\{2\}^b}^f \right. \\ \left. + 2 q_{tx}^2 q_{ub} q_{uf} q_{ur} P_{ur/\{1\}^f}^b \bar{P}_{ud}^b P_{ur/\{1\}^b}^f \bar{P}_{rd/\{1\}^b}^f \right]. \quad (36)$$

## APPENDIX D

Hereafter, we analyze the performance of the queue at the relay for  $N$  UEs. First, we compute the average arrival rate that is given by:

$$\lambda_r = P(Q = 0) \lambda_r^0 + P(Q \neq 0) \lambda_r^1 = P(Q = 0) \sum_{k=1}^N k r_k^0 + P(Q \neq 0) \sum_{k=1}^N k r_k^1, \quad (37)$$

where,  $r_k^0$  and  $r_k^1$  are the probabilities that  $R$  receives  $k$  packets in a timeslot when the queue is empty or not. These events occur with probabilities  $P(Q = 0)$  and  $P(Q \neq 0)$ , respectively, and are derived in the end of this appendix. In order to compute  $r_k^0$  and  $r_k^1$ , we indicate with  $m$  out of  $N$  the number of UEs that transmit a packet, with  $i$  (at most  $m$ ) the number of transmitting UEs that use FD transmissions ( $m - i$  UEs use the BR transmission), and with  $j$  the number of FD UEs that transmit to  $R$  ( $i - j$  UEs transmit to the mmAP). Moreover,  $k$  is the total number of packets successfully received by the relay in a timeslot, and  $k_f$  out of them are received by using FD transmissions ( $k - k_f$  packets are received by using a BR transmission). Thus, we can express  $r_k^0$  and  $r_k^1$  as follows:

$$r_k^0 = \sum_{m=k}^N \binom{N}{m} q_{tx}^m \bar{q}_{tx}^{N-m} \sum_{i=0}^m \binom{m}{i} q_{uf}^i q_{ub}^{m-i} \sum_{j=\max(0, k+i-m)}^i \binom{i}{j} q_{ur}^j q_{um}^{i-j} \sum_{k_f=\max(0, k+i-m)}^{\min(j, k)} \binom{j}{k_f} \\ \times (P_{ur/\{j-1\}^f, \{m-i\}^b}^f)^{k_f} (\bar{P}_{ur/\{j-1\}^f, \{m-i\}^b}^f)^{j-k_f} \times \binom{m-i}{k-k_f} (P_{ur/\{j\}^f, \{m-i-1\}^b}^b \bar{P}_{ud/\{i-j\}^f, \{m-i-1\}^b}^b)^{k-k_f} \\ \times (1 - P_{ur/\{j\}^f, \{m-i-1\}^b}^b \bar{P}_{ud/\{i-j\}^f, \{m-i-1\}^b}^b)^{m-i-k+k_f}, \quad (38)$$

$$r_k^1 = \bar{q}_r r_k^0 + q_r \sum_{m=k}^N \binom{N}{m} q_{tx}^m \bar{q}_{tx}^{N-m} \sum_{i=0}^m \binom{m}{i} q_{uf}^i q_{ub}^{m-i} \sum_{j=\max(0, k+i-m)}^i \binom{i}{j} q_{ur}^j q_{um}^{i-j} \sum_{k_f=\max(0, k+i-m)}^{\min(j, k)} \binom{j}{k_f} \\ \times (P_{ur/\{j-1\}^f, \{m-i\}^b}^f)^{k_f} (\bar{P}_{ur/\{j-1\}^f, \{m-i\}^b}^f)^{j-k_f} \binom{m-i}{k-k_f} (P_{ur/\{j\}^f, \{m-i-1\}^b}^b \bar{P}_{ud/\{i-j, r\}^f, \{m-i-1\}^b}^b)^{k-k_f} \\ \times (1 - P_{ur/\{j\}^f, \{m-i-1\}^b}^b \bar{P}_{ud/\{i-1, r\}^f, \{m-i-1\}^b}^b)^{m-i-k+k_f}. \quad (39)$$

Then, we derive the relay's service rate  $\mu_R$ , which is given by:

$$\mu_r = q_r \sum_{m=0}^N \binom{N}{m} q_{tx}^m \bar{q}_{tx}^{N-m} \sum_{i=0}^m \binom{m}{i} q_{uf}^m q_{ub}^{N-m} \sum_{j=0}^i \binom{i}{j} q_{ur}^j q_{um}^{i-j} P_{rd/\{i-j\}^f, \{m-i\}^b}^f, \quad (40)$$

Now, we can study the evolution of the queue at  $R$  by using a discrete time Markov Chain, whose transition matrix is a lower Hessenberg matrix given by:

$$\begin{pmatrix} a_0 & b_0 & 0 & 0 & \dots \\ a_1 & b_1 & b_0 & 0 & \dots \\ a_2 & b_2 & b_1 & b_0 & \dots \\ a_3 & b_3 & b_2 & b_1 & \dots \\ a_4 & b_4 & b_3 & b_2 & \dots \\ \vdots & \vdots & \vdots & \vdots & \ddots \end{pmatrix}. \quad (41)$$

The elements of the matrix are represented by  $a_k = p_k^0$ ,  $b_0 = p_{-1}^1$ ,  $b_1 = p_0^1$ , and  $b_{k+1} = p_k^1$   $\forall k > 0$ . The terms  $p_k^0$  and  $p_k^1$  are the probabilities that the queue size increases by  $k$  packets in a timeslot when the queue is empty or not. By using the same notation as in (38), these terms can be written as follows:

$$p_k^0 = r_k^0, \quad (42)$$

$$\begin{aligned} p_{-1}^1 &= q_r \sum_{m=0}^N \binom{N}{m} q_{tx}^m \bar{q}_{tx}^{N-m} \sum_{i=0}^m \binom{m}{i} q_{uf}^i q_{ub}^{m-i} \sum_{j=0}^i \binom{i}{j} q_{ur}^j q_{um}^{i-j} P_{rd/\{i-j\}^f, \{m-i\}^b}^f \left( \bar{P}_{ur/\{j-1\}^f, \{m-i\}^b}^f \right)^j \\ &\times (1 - P_{ur/\{j\}^f, \{m-i-1\}^b}^b \bar{P}_{ud/\{i-j, r\}^f, \{m-i-1\}^b}^b)^{m-i}, \end{aligned} \quad (43)$$

$$\begin{aligned} p_k^1 &= \bar{q}_r r_k^0 + q_r \sum_{m=k}^N \binom{N}{m} q_{tx}^m \bar{q}_{tx}^{N-m} \sum_{i=0}^m \binom{m}{i} q_{uf}^i q_{ub}^{m-i} \sum_{j=\max(0, k+i-m)}^i \binom{i}{j} q_{ur}^j q_{um}^{i-j} \sum_{k_f=\max(0, k+i-m)}^{\min(j, k)} \binom{j}{k_f} \\ &\times (P_{ur/\{j-1\}^f, \{m-i\}^b}^f)^{k_f} (\bar{P}_{ur/\{j-1\}^f, \{m-i\}^b}^f)^{j-k_f} \times \binom{m-i}{k-k_f} (P_{ur/\{j\}^f, \{m-i-1\}^b}^b \bar{P}_{ud/\{i-j, r\}^f, \{m-i-1\}^b}^b)^{k-k_f} \\ &\times (1 - P_{ur/\{j\}^f, \{m-i-1\}^b}^b \bar{P}_{ud/\{i-j, r\}^f, \{m-i-1\}^b}^b)^{m-i-k+k_f} \bar{P}_{rd/\{i-j\}^f, \{m-i\}^b}^f + q_r \sum_{m=k+1}^N \binom{N}{m} q_{tx}^m \bar{q}_{tx}^{N-m} \\ &\times \sum_{i=0}^m \binom{m}{i} q_{uf}^i q_{ub}^{m-i} \sum_{j=\max(0, k+1+i-m)}^i \binom{i}{j} q_{ur}^j q_{um}^{i-j} \sum_{k_f=\max(0, k+1+i-m)}^{\min(j, k+1)} \binom{j}{k_f} \binom{m-i}{k+1-k_f} \\ &\times (P_{ur/\{j-1\}^f, \{m-i\}^b}^f)^{k_f} (\bar{P}_{ur/\{j-1\}^f, \{m-i\}^b}^f)^{j-k_f} (P_{ur/\{j\}^f, \{m-i-1\}^b}^b \bar{P}_{ud/\{i-j, r\}^f, \{m-i-1\}^b}^b)^{k+1-k_f} \\ &\times (1 - P_{ur/\{j\}^f, \{m-i-1\}^b}^b \bar{P}_{ud/\{i-j, r\}^f, \{m-i-1\}^b}^b)^{m-i-k-1+k_f} P_{rd/\{i-j\}^f, \{m-i\}^b}^f, \end{aligned} \quad (44)$$

$$p_0^1 = 1 - p_{-1}^1 - \sum_{k=1}^N N p_k^1. \quad (45)$$

Finally, we can compute the probability that the queue is empty,  $P(Q = 0)$ , and the average relay queue size,  $\bar{Q}$ . Hereafter, we show the main steps of the derivations that are illustrated with more details in [36]. First, we can note that the queue at  $R$  can be modelled as an  $M^N/M/1$  queue, therefore, the equation that describes the evolution of the states is given by:

$$s_i = a_i s_0 + \sum_{j=1}^{i+1} b_{i-j+1} s_j, \quad (46)$$

where,  $s_i$  represents the probability of finding our system in state  $i$  at equilibrium. Let  $s$  be the steady-state distribution vector and  $S(z)$  its Z-transformation, we have:

$$S(z) = \sum_{i=1}^{\infty} s_i z^{-i} \Rightarrow \bar{Q} = -S'(1) = -s_0 \frac{K''(1)}{L''(1)}. \quad (47)$$

The terms  $K''(z)$  and  $L''(z)$  in (47) are the second derivatives of  $K(z)$  and  $L(z)$ , respectively. These are given by [36]:

$$\begin{aligned} K(z) &= (-z^{-2} A(z) + z^{-1} A'(z) - B'(z))(z^{-1} - B(z)) \\ &\quad - (z^{-1} A'(z) - B(z))(-z^{-2} - B'(z)), \end{aligned} \quad (48)$$

$$L(z) = (z^{-1} - B(z))^2, \quad (49)$$

where,  $A(z) = \sum_{i=1}^N a_i z^{-i}$  and  $B(z) = \sum_{i=1}^{N+1} b_i z^{-i}$  ( $a_i$  and  $b_i$  are the elements of the transition matrix (41)). The term  $s_0$ , in (47), is the probability that the queue is empty at equilibrium, which can be written as follows [36]:

$$P(Q = 0) = \frac{1 + B'(1)}{1 + B'(1) - A'(1)}. \quad (50)$$

Then, by replacing the first derivative of  $A(z)$  and  $B(z)$  in (50), we obtain:

$$P(Q = 0) = \frac{p_{-1}^1 - \sum_{i=1}^N i p_i^1}{p_{-1}^1 - \sum_{i=1}^N i p_i^1 + \lambda_r^0}. \quad (51)$$

Finally, by considering (47), (48), (49), and (51), we can express  $\bar{Q}$  as follows:

$$\bar{Q} = \frac{\left(\sum_{k=1}^N k p_k^1 - p_{-1}^1\right) \sum_{k=1}^N k(k+3) p_k^0 + \lambda_r^0 \left(2 p_{-1}^1 - \sum_{k=1}^N k(k+3) p_k^1\right)}{2 \left(\sum_{k=1}^N k p_k^1 - p_{-1}^1\right) \left(p_{-1}^1 - \sum_{k=1}^N N k p_k^1 + \lambda_r^0\right)}. \quad (52)$$

## REFERENCES

- [1] C. Tatino, N. Pappas, I. Malanchini, L. Ewe, and D. Yuan, "Throughput analysis for relay-assisted millimeter-wave wireless networks," *to appear at GLOBECOM Workshops*, 2018. [Online]. Available: <http://arxiv.org/abs/1804.09450>
- [2] E. Hossain and M. Hasan, "5G cellular: key enabling technologies and research challenges," *IEEE Instrumentation Measurement Magazine*, vol. 18, no. 3, pp. 11–21, June 2015.
- [3] T. S. Rappaport, Y. Xing, G. R. MacCartney, A. F. Molisch, E. Mellios, and J. Zhang, "Overview of millimeter wave communications for fifth-generation (5G) wireless networks-with a focus on propagation models," *IEEE Transactions on Antennas and Propagation*, vol. 65, no. 12, pp. 6213–6230, Dec. 2017.
- [4] H. Zhao, R. Mayzus, S. Sun, M. Samimi, J. K. Schulz, Y. Azar, K. Wang, G. N. Wong, F. Gutierrez, and T. S. Rappaport, "28 GHz millimeter wave cellular communication measurements for reflection and penetration loss in and around buildings in new york city," in *IEEE International Conference on Communications (ICC)*, June 2013, pp. 5163–5167.
- [5] G. R. MacCartney and T. S. Rappaport, "73 GHz millimeter wave propagation measurements for outdoor urban mobile and backhaul communications in new york city," in *IEEE International Conference on Communications (ICC)*, June 2014, pp. 4862–4867.
- [6] Y. Niu, Y. Li, D. Jin, L. Su, and A. V. Vasilakos, "A survey of millimeter wave communications (mmwave) for 5g: Opportunities and challenges," *Wireless Networks*, vol. 21, no. 8, pp. 2657–2676, Nov. 2015. [Online]. Available: <https://doi.org/10.1007/s11276-015-0942-z>
- [7] C. Tatino, I. Malanchini, D. Aziz, and D. Yuan, "Beam based stochastic model of the coverage probability in 5G millimeter wave systems," in *the 15th International Symposium on Modeling and Optimization in Mobile, Ad Hoc, and Wireless Networks (WiOpt)*, May 2017, pp. 1–6.
- [8] D. Moltchanov, A. Ometov, S. Andreev, and Y. Koucheryavy, "Upper bound on capacity of 5G mmwave cellular with multi-connectivity capabilities," *Electronics Letters*, vol. 54, no. 11, pp. 724–726, 2018.
- [9] C. Tatino, I. Malanchini, N. Pappas, and D. Yuan, "Maximum throughput scheduling for multi-connectivity in millimeter-wave networks," in *the 16th International Symposium on Modeling and Optimization in Mobile, Ad Hoc, and Wireless Networks (WiOpt)*, May 2018, pp. 1–6.
- [10] G. Kramer, I. Marić, and R. D. Yates, "Cooperative communications," *Found. Trends Netw.*, vol. 1, no. 3, pp. 271–425, Aug. 2006.
- [11] A. K. Sadek, K. J. R. Liu, and A. Ephremides, "Cognitive multiple access via cooperation: Protocol design and performance analysis," *IEEE Transactions on Information Theory*, vol. 53, no. 10, pp. 3677–3696, Oct. 2007.
- [12] B. Rong and A. Ephremides, "Cooperative access in wireless networks: Stable throughput and delay," *IEEE Transactions on Information Theory*, vol. 58, no. 9, pp. 5890–5907, Sept. 2012.
- [13] O. Simeone, Y. Bar-Ness, and U. Spagnolini, "Stable throughput of cognitive radios with and without relaying capability," *IEEE Transactions on Communications*, vol. 55, no. 12, pp. 2351–2360, Dec 2007.
- [14] N. Pappas, A. Ephremides, and A. Traganitis, "Relay-assisted multiple access with multi-packet reception capability and simultaneous transmission and reception," in *IEEE Information Theory Workshop*, Oct. 2011, pp. 578–582.
- [15] N. Pappas, M. Kountouris, A. Ephremides, and A. Traganitis, "Relay-assisted multiple access with full-duplex multi-packet reception," *IEEE Transactions on Wireless Communications*, vol. 14, no. 7, pp. 3544–3558, July 2015.
- [16] G. Papadimitriou, N. Pappas, A. Traganitis, and V. Angelakis, "Network-level performance evaluation of a two-relay cooperative random access wireless system," *Computer Networks*, vol. 88, pp. 187–201, Sept. 2015.
- [17] N. Nomikos, T. Charalambous, I. Krikidis, D. N. Skoutas, D. Vouyioukas, M. Johansson, and C. Skianis, "A survey on buffer-aided relay selection," *IEEE Communications Surveys Tutorials*, vol. 18, no. 2, pp. 1073–1097, Secondquarter 2016.

- [18] M. Giordani, M. Mezzavilla, and M. Zorzi, "Initial access in 5G mmwave cellular networks," *IEEE Communications Magazine*, vol. 54, no. 11, pp. 40–47, Nov. 2016.
- [19] C. N. Barati, S. A. Hosseini, M. Mezzavilla, T. Korakis, S. S. Panwar, S. Rangan, and M. Zorzi, "Initial access in millimeter wave cellular systems," *IEEE Transactions on Wireless Communications*, vol. 15, no. 12, pp. 7926–7940, Dec. 2016.
- [20] V. K. Sakarellos, D. Skraparlis, A. D. Panagopoulos, and J. D. Kanellopoulos, "Cooperative diversity performance in millimeter wave radio systems," *IEEE Transactions on Communications*, vol. 60, no. 12, pp. 3641–3649, Dec. 2012.
- [21] B. Xie, Z. Zhang, and R. Q. Hu, "Performance study on relay-assisted millimeter wave cellular networks," in *IEEE 83rd Vehicular Technology Conference (VTC Spring)*, May 2016, pp. 1–5.
- [22] S. Biswas, S. Vuppala, J. Xue, and T. Ratnarajah, "On the performance of relay aided millimeter wave networks," *IEEE Journal of Selected Topics in Signal Processing*, vol. 10, no. 3, pp. 576–588, Apr. 2016.
- [23] X. Lin and J. G. Andrews, "Connectivity of millimeter wave networks with multi-hop relaying," *IEEE Wireless Communications Letters*, vol. 4, no. 2, pp. 209–212, April 2015.
- [24] K. Belbase, Z. Zhang, H. Jiang, and C. Tellambura, "Coverage analysis of millimeter wave decode-and-forward networks with best relay selection," *IEEE Access*, vol. 6, pp. 22 670–22 683, 2018.
- [25] N. Wei, X. Lin, and Z. Zhang, "Optimal relay probing in millimeter-wave cellular systems with device-to-device relaying," *IEEE Transactions on Vehicular Technology*, vol. 65, no. 12, pp. 10 218–10 222, Dec. 2016.
- [26] S. Wu, R. Atat, N. Mastronarde, and L. Liu, "Coverage analysis of d2d relay-assisted millimeter-wave cellular networks," in *IEEE Wireless Communications and Networking Conference (WCNC)*, Mar. 2017, pp. 1–6.
- [27] J. W. Sungoh Kwon, "Relay selection for mmwave communications," in *the 28th Annual IEEE International Symposium on Personal, Indoor and Mobile Radio Communications (IEEE PIMRC)*, Oct. 2017, pp. 1–5.
- [28] Y. Xu, H. Shokri-Ghadikolaei, and C. Fischione, "Distributed association and relaying with fairness in millimeter wave networks," *IEEE Transactions on Wireless Communications*, vol. 15, no. 12, pp. 7955–7970, Dec. 2016.
- [29] R. Congiu, H. Shokri-Ghadikolaei, C. Fischione, and F. Santucci, "On the relay-fallback tradeoff in millimeter wave wireless system," in *IEEE Conference on Computer Communications Workshops (INFOCOM WKSHPS)*, Apr. 2016, pp. 622–627.
- [30] N. Pappas, I. Dimitriou, and Z. Cheng, "Network-level cooperation in random access iot networks with aggregators," in *30th International Teletraffic Congress (ITC 30)*, vol. 1, Sept. 2018.
- [31] S. Sun, T. S. Rappaport, R. W. Heath, A. Nix, and S. Rangan, "Mimo for millimeter-wave wireless communications: beamforming, spatial multiplexing, or both?" *IEEE Communications Magazine*, vol. 52, no. 12, pp. 110–121, Dec. 2014.
- [32] H. Shokri-Ghadikolaei and C. Fischione, "The transitional behavior of interference in millimeter wave networks and its impact on medium access control," *IEEE Transactions on Communications*, vol. 64, no. 2, pp. 723–740, Feb. 2016.
- [33] T. Bai and R. W. Heath, "Coverage and rate analysis for millimeter-wave cellular networks," *IEEE Transactions on Wireless Communications*, vol. 14, no. 2, pp. 1100–1114, Feb. 2015.
- [34] R. M. Loynes, "The stability of a queue with non-independent inter-arrival and service times," *Mathematical Proceedings of the Cambridge Philosophical Society*, vol. 58, no. 3, pp. 497–520, 1962.
- [35] 3GPP, "Study on channel model for frequencies from 0.5 to 100 GHz (release 14), 3gpp tr 38.901 v14.2.0," Tech. Rep., Sept. 2017.
- [36] F. Gebali, *Analysis of Computer and Communication Networks*. New York, NY, USA: Springer-Verlag, 2010.